Review of Porosity Distributions in the Yucca Mountain Region

Prepared for

Nuclear Regulatory Commission
Contract NRC–02–97–009

Prepared by

David A. Farrell
James Winterle
Walter A. Illman
Randall W. Fedors

Center for Nuclear Waste Regulatory Analyses
San Antonio, Texas

April 2000

ABSTRACT

Integral components of the performance assessment of the proposed high-level waste repository at Yucca Mountain (YM), Nevada, are evaluation of the hydrogeologic system and its influence on radionuclide migration away from the site. One aspect of the hydrogeologic system considered important to both groundwater flow and radionuclide transport, at and away from the site, is effective porosity. This report presents a review of information regarding the distribution of porosity at YM. In particular, this report examines the quality and quantity of effective porosity data at the site and remaining uncertainties regarding these data. For the surficial deposits at YM, estimated effective matrix porosities may be biased by sampling procedures leading to overestimations in porosity and soil storage capacity and thus underestimations of infiltration and deep percolation. In the unsaturated zone (UZ), effective matrix porosities are used to categorize the geologic units. Within this zone, deep percolation is influenced by the distributions of effective matrix and fracture porosities. Measured effective matrix porosities in the UZ appear well constrained with the possible exception of the vitric units of the Calico Hills Formation, which have been sparsely sampled. Effective fracture and fault properties within the UZ are poorly constrained largely because of limited numbers of interpreted pneumatic and gas tracer-tests. Changes in effective porosities that may occur during the postclosure period due to thermal and mechanical loading are currently poorly understood and as a result, poorly constrained. Effective porosity estimates for the tuff units in the saturated zone appear to be reasonably well constrained. Few estimates of porosity are available for the valley-fill units south of YM. Those that are available are not based on field measurements. In addition to reporting on effective porosities at the site, this report presents discussions that (i) highlight the importance of effective porosity to groundwater flow and radionuclide transport, and (ii) summarize the various approaches for estimating effective porosities.

3/36

CONTENTS

CONTENTS (cont'd)

4/36

FIGURES

5/3L

TABLES

4/36

ACKNOWLEDGMENTS

This report was prepared to document work performed by the Center for Nuclear Waste Regulatory Analyses (CNWRA) for the Nuclear Regulatory Commission (NRC) under Contract No. NRC–02–97–009. The activities reported here were performed on behalf of the NRC Office of Nuclear Material Safety and Safeguards, Division of Waste Management. The report is an independent product of the CNWRA and does not necessarily reflect the views or regulatory position of the NRC.

The authors wish to thank Gordon Wittmeyer for his thorough technical review, Barbara Long for her editorial expertise, Budhi Sagar for programmatic review, and Janet Wike for format review. Also appreciated is Paulette Houston for staff support.

QUALITY OF DATA, ANALYSES, AND CODE DEVELOPMENT

DATA: CNWRA-generated original data contained in this report meet quality assurance requirements described in the CNWRA Quality Assurance Manual. Sources for other data should be consulted for determining the level of quality for those data.

ANALYSES AND CODES: No computer codes were used for analyses contained in this report.

1 INTRODUCTION

Yucca Mountain (YM), Nye County, Nevada, located approximately 135 km northwest of Las Vegas, Nevada, is currently being considered by the U.S. Department of Energy (DOE) as a potential site for high-level waste (HLW) repository. The current design stipulates that the waste be placed in corrosion resistant canisters prior to emplacement in drifts located within unsaturated tuffs at the site. In 2001 the DOE is expected to submit to the Nuclear Regulatory Commission (NRC) a license application that makes the case that the facility poses no health risk to the surrounding environment. A key evaluation affecting licensing of the repository by NRC is whether the engineered containment system and the natural barrier system provided by the geologic and hydrogeologic environments will provide effective long-term isolation of the waste from the accessible biosphere. Should the engineered barrier system fail, radionuclides potentially could be transported by percolating groundwater through the unsaturated zone (UZ) to the saturated zone (SZ) and subsequently transported by the regional groundwater system to potential users.

To demonstrate that the proposed repository poses no health risk to the surrounding biosphere, the DOE developed an integrated repository performance assessment (PA) model to simulate the expected dynamics of the repository system and its potential impacts on the surrounding biosphere (Civilian Radioactive Waste Management System, Management and Operating Contractor, 1998). The NRC also has independently developed its own PA model to simulate the expected dynamics of the repository system and its potential impacts on the surrounding biosphere (Mohanty and McCartin, 1998). Within the PA framework, process models representing various physical phenomena at the site, or abstracted results from such models are used. Among the processes represented in the PA models are site hydrogeology and radionuclide transport.

Estimation of groundwater flow velocities, radionuclide transport pathways, radionuclide transport times to compliance points, and radionuclide concentrations at such locations, which are essential functions of PA models, are strongly influenced by the porosity of the hydrogeologic media through which flow and transport occur. Because of the complexity and variability of the geologic processes that have occurred at the site throughout geologic time, the distribution of porosity at the site is highly heterogeneous, ranging from less that 1 percent in the densely welded units to greater than 50 percent in the poorly welded volcanic units (Flint, 1998). An indepth discussion of this heterogeneity is reserved for later sections of this report.

The importance of porosity on repository performance has been investigated to varying degrees by the DOE and the NRC. Using the Total-system Performance Assessment (TPA) Version 3.2 code, NRC performed a series of sensitivity analyses to look at the relative importance of model parameters on repository performance. The analyses showed that for the basecase, the effective porosity of the saturated alluvium south of the repository ranked among the top 20 model parameters influencing repository performance after both 10,000 and 50,000 yrs (Mohanty et al., 1999, tables 4-1 and 4-2). In the DOE Viability Assessment (VA), effective porosity was identified as one of the transport parameters that should be given high priority (Civilian Radioactive Waste Management System, Management and Operating Contractor, 1998, table 3-19).

Because of its documented importance to repository performance, this report provides a critical review of the current knowledge of porosity in the Yucca Mountain region (YMR), with the ultimate goal of establishing a basis for the geologic unit porosity values currently used in groundwater flow, and mass transport simulations for the region, and repository PA simulations. Where appropriate, approaches to better constrain porosity estimates are suggested. In addition, regions that require further characterization to better constrain porosity estimates are identified.

The format of this report is as follows. Chapter 2 provides a general introduction to the concept of porosity and is meant to serve as a reference for current and future discussions and reviews of porosity. The chapter discusses various definitions of porosity commonly seen in literature and their relevance to groundwater flow and mass transport. This chapter also includes brief summaries of the various methods commonly employed to estimate porosity, along with advantages and disadvantages. Chapter 3 provides a brief review of the geology and hydrogeology of the region that gives a general framework for discussions of porosity heterogeneity at the site. Chapter 4 presents a critical review of the porosity estimates for the various geologic units extending from the ground surface above the repository footprint to the water table and along the projected radionuclide flowpaths from the repository footprint to compliance points to the south. To be consistent with a recent report on permeability at YM (Winterle et al., 2000), this chapter is subdivided into two sections: review of porosity in the UZ and review of porosity in the SZ. Chapter 5 summarizes the general findings of this report and discusses further work needed to resolve outstanding concerns.

2 INTRODUCTION TO POROSITY

2.1 INTRODUCTION

This chapter provides a foundation for the discussions of porosity contained in subsequent chapters. The material presented in this chapter may be used either as a guide for future reviews of porosity at the YM site or as a reference for determining suitable methods of estimating porosity at the site.

The first part of the chapter presents detailed definitions of porosity and related quantities, such as effective porosity, that are often encountered when reviewing literature on YM. These definitions are followed by a discussion of the importance of porosity on groundwater flow and mass transport processes. Next, a summary of approaches for estimating porosity is presented. The chapter concludes with a summary of the material discussed.

2.2 DEFINING POROSITY

The total porosity, φ, of a rock or soil sample is defined as the ratio of the volume of void space in the sample, V_v, to the bulk volume of the sample, V_t, (i.e., $\varphi = V_v/V_t$). Comprehensive summaries of the ranges of porosities reported for most geologic material are summarized in Freeze and Cherry (1979, page 37, table 2.4; cf., Davis, 1969) and Domenico and Schwartz (1990, page 26, table 2.1). The tables show that porosities reported for geologic material range between 0 and 70 percent, with dense crystalline rocks having the lowest porosities (0–5 percent) and clays possessing the highest porosities (40–70 percent). In general, rocks have lower porosities than soils; gravel, sands, and silts, composed of angular particles, have lower porosities than soils rich in platy minerals; and poorly sorted deposits have lower porosities than well-sorted deposits (Freeze and Cherry, 1979).

Two classes of porosity are commonly referenced in literature–primary porosity and secondary porosity. Primary porosity (or interstitial porosity) is solely due to the soil or rock matrix (Freeze and Cherry, 1979). Secondary porosity describes the porosity that develops because of alteration of the porous medium after its deposition or emplacement. This alteration may be caused by solution processes, producing for example caves in limestone systems, or tectonic processes, producing fractures in rock masses. Secondary porosity may either significantly enhance groundwater flow and mass transport processes in an otherwise impermeable unit or it may significantly reduce these processes in an otherwise highly porous medium.

When describing porosity, another distinction often drawn is the difference between total porosity and effective porosity. Total porosity does not differentiate between interconnected and disconnected pores, whereas effective porosity describes only the interconnected pore space. As pointed out by Domenico and Schwartz (1990), many rocks, crystallines in particular, have a high total porosity, most of which is unconnected. Effective porosity describes connectivity of pore spaces through the solid medium and is, therefore, more closely correlated to permeability than total porosity (Domenico and Schwartz, 1990). As demonstrated by Domenico and Schwartz (1990, page 26, table 2.2), effective porosity can be more than one magnitude smaller than total porosity, with the greatest difference occurring in fractured rocks. It is important to note that from the perspectives of groundwater flow and mass transport, effective porosity is often used to refer to the "mobile regions" of the system where groundwater flow occurs, while the remainder of the porosity, excluding the effective porosity, sometimes termed the "immobile region", accommodates negligible groundwater flow. From the perspective of mass transport, however, both the mobile and immobile

regions may be linked by diffusive mass transfer processes (Brusseau et al., 1989). In such systems, the immobile regions act as distributed sources and sinks for the transported mass. Mass transport, as described by solute breakthrough curves in such systems, is characterized by early initial breakthrough resulting from rapid transport along the advective pathways and by tailing (i.e., delayed approach to relative concentration values of 0 or 1) (Brusseau et al., 1989).

The relationship between total porosity and effective porosity is analogous to the relationship between permeability and hydraulic conductivity. Because total porosity does not differentiate between interconnected and disconnected pore spaces, it is an intrinsic property of porous media much like permeability. However, as demonstrated by field and laboratory studies of solute transport (cf., Peyton et al., 1985; de Marsily, 1986), effective porosity is not an intrinsic soil parameter applicable to all solutes in all groundwater flow conditions (Peyton et al., 1985) and, therefore, by analogy, should be viewed in a similar manner as hydraulic conductivity, which is not dependent only on the properties of the porous medium but also the properties of the migrating fluid. Peyton et al. (1985) suggested that effective porosity may be defined better based on the void volume available to a particular solute species and the flow regime. The latter suggests that effective porosity is to some degree a site specific parameter. If this is the case, then from a practical standpoint it is desirable to estimate effective porosity under conditions that approximate as closely as possible those present in the ambient groundwater system at the site of interest. To reflect this dynamic nature, dynamic porosity is sometimes used to define porosities estimated under differing flow conditions. In low velocity groundwater flow systems where equilibrium conditions can be assumed, dynamic porosity generally attains a limiting value that is based solely on molecular size to pore size distribution. Under these conditions, the limiting value represents the effective porosity of the medium for the system.

Specific yield is occasionally used interchangeably with porosity. According to Fetter (1994), total porosity is the sum of two quantities, the specific yield and the specific retention, where the specific yield, S_y, refers to the ratio of the volume of water that drains from a saturated rock due to gravity, V_{wl}, to the total volume of the rock, $S_y = V_{wl}/V_t$. Specific retention, S_r, refers to the volume of water a rock can retain against gravity drainage, V_{wr}, to the total volume of the rock, $S_r = V_{wr}/V_t$. As a general rule, specific retention increases with decreasing grain size (Fetter, 1994), so that using Fetter's definition, the specific yield for most soils will underestimate total porosity, with the underestimation increasing for finer grained soils. A slightly different relationship between total porosity and specific yield has been proposed by Domenico and Schwartz (1990). With their definition, the specific retention refers to water that remains in the drainable pore space after gravity drainage; hence, total porosity becomes the sum of the specific yield, the specific retention, and the ratio of the dead-end void space to the bulk volume. Using this definition, it is reasonable to equate effective porosity to specific yield, particularly for coarse grained material where the specific retention is small.

2.3 IMPORTANCE OF POROSITY ON GROUNDWATER FLOW AND MASS TRANSPORT MODELS

Effective porosity, φ_{ef}, is an important parameter in the calculation of the average linear groundwater velocity (groundwater pore velocity), v, where $v = q/\varphi_{ef}$ with q the specific discharge calculated by application of Darcy's law to the hydraulic head field. For conservative solutes, v allows estimation of the advective travel time, $t = x/v = x\varphi_{ef}/q$, of the center of mass of a solute plume associated with a pulse source or the 0.5 relative concentration contour for a plume based on a continuous source. Here, x represents the advective travel distance. As shown, the advective travel time is proportional to the effective porosity.

That is, as the effective porosity increases (assuming no correlation between hydraulic conductivity and effective porosity) so too does the advective travel time. In the context of YM, this implies that if a conservative tracer is released at the repository location, then the advective travel time of the tracer from the source to compliance points will increase with increasing effective porosity.

Effective porosity may also be used to estimate moisture storage in unconfined aquifer systems, such as the valley-fill aquifer system south of YM. In such systems, effective porosity may be used as the upper limit for specific yield (see section 2.2). For confined aquifer systems, the impacts of effective porosity of aquifer storage are much less pronounced and generally overwhelmed by the compressibility of the porous medium. In cases where correlations exist between saturated hydraulic conductivity and effective porosity, the latter may be used to infer the former. In the UZ, effective porosities are important because they form limiting values for soil moisture content that are used to estimate quantities such as infiltration and deep percolation rates.

Effective porosity is an important parameter in the solution of the mass transport equation where it contributes, via the velocity term, to both the advective and dispersive components (e.g., Bear and Verruijt, 1987). As such, failure to properly account for the effective porosity in the advective and dispersive components of the mass transport equation can result in significant over- or underestimations of solute concentrations at down-gradient compliance points.

Effective porosity may also affect solute migration via its influence on the adsorption of mass onto mineral surfaces contained in the solid matrix. In this way the solid matrix acts as a concentration sink and results in retardation of solute migration. Here, retardation, R, is defined as the ratio of the groundwater velocity, v, to the velocity of the solute, v_c, (i.e., $R = v/v_c$). The amount of retardation occurring in this manner is controlled in part by the ratio of the mineral surface area within the porous medium to the pore volume, which generally correlates to the porosity of the medium. The distribution of mobile to immobile pore spaces also affects solute retardation. Where diffusive mass transfer between these two regions occurs, waters in immobile pore zones may act as concentration sinks.

A recent, elaborate and informative discussion on the importance of porosity on solute transport in porous media is provided by Hassan et al. (1998). The authors examined the impact of random hydraulic conductivity, porosity, and geochemical variability on conservative and reactive solute transport using a numerical simulation approach. In summary, their results showed that when porosity is correlated to hydraulic conductivity, the dispersion process is significantly impacted with positive correlation resulting in decreased longitudinal dispersion and negative correlation resulting in increased longitudinal dispersion. In both cases, the impacts on transverse dispersion were viewed as minimal. In the analysis, dispersion is referenced to the case of zero correlation. For reactive transport in physically and chemically heterogeneous media, the authors found that combining variability in porosity with geochemical variability significantly affected transport, with the relative importance of each variable controlled by the degree of heterogeneity present in each field. In the context of YM, these results may be of importance, particularly for the heterogeneous valley-fill units, and suggest that careful characterization and identification of possible correlations between hydraulic and geochemical parameters at the site may be required.

2.4 APPROACHES FOR ESTIMATING POROSITY

To gain a better understanding of the porosity data presented in the following chapters and its potential limitations, a summary of the various approaches available for estimating porosity is provided. However, because most of this material is essentially for reference and review, discussions of these methods are restricted to the appendix of this report. It should be noted that the summary presented in the appendix is not restricted to methods applied in the YMR. As a result, the summary can be used to guide future attempts to estimate the porosity of materials in the YMR and possible review methods for porosity data.

2.5 CORE-SCALE EFFECTIVE POROSITY ESTIMATES VERSUS FIELD-SCALE EFFECTIVE POROSITY ESTIMATES

As illustrated in the appendix, effective porosity may be measured at varying scales ranging from the core-scale (fractions of meters) to the field-scale (tens to hundreds of meters). Effective porosity values measured on the core-scale are representative of local phenomena and therefore may not be representative of the range of porosities within geologic formations. Effective porosities measured on the field-scale, in particular those estimated using tracer-tests, generally incorporate more formation heterogeneity and as a result, may be more representative of formation porosities. However, for large tracer-tests conducted in heterogeneous environments, the estimated effective porosity may represent a lumped or fitted parameter reflecting contributions from several geologic units of differing effective porosity and geometry. For groundwater and mass transport simulations in heterogeneous environments, this lumped parameter is commonly used for effective porosity. Because core-scale and field-scale (formation-scale) porosities may differ, combining these porosities in datasets for groundwater flow and mass transport simulations without appropriate regularization can lead to prediction errors of hydraulic head and solute concentration.

2.6 SUMMARY

Chapter 2 provided an overview of porosity and its effects on groundwater flow and solute transport processes. Of particular importance to these processes are effective primary and secondary porosities. Effective porosity is important for groundwater flow because it controls (i) groundwater velocities, (ii) the amount of moisture that can be stored by the porous media, and (iii) infiltration rates. With regard to solute transport processes, porosity is important because it controls (i) advective solute velocities, (ii) dispersive processes, and (iii) geochemical partitioning processes that may lead to attenuation of solute concentrations. State of the art approaches for estimating porosity of porous media were introduced in this chapter, and are discussed in detail in the appendix of this report.

3 SITE DESCRIPTION

This chapter summarizes aspects of the geology and hydrogeology of the YMR deemed pertinent to laying the groundwork for discussions of porosity distribution in the region. Comprehensive discussions of the material summarized in this chapter are contained in Farrell et al. (1999), Day et al. (1998a,b), and Luckey et al. (1996) among others.

Figure 3-1 identifies the region of primary interest for this report. This region includes the southern part of the Nevada Test Site (NTS), the area immediately west of the NTS including YM and extending to Crater Flat, and the area south of the NTS extending into the northern portion of the Amargosa Desert.

3.1 STRATIGRAPHIC SETTING

Rocks of the YMR consist of thick accumulations (15 km in some places) of Neoproterozoic and Phanerozoic sedimentary and igneous rocks resting on structurally complex crystalline basement mainly composed of gneiss, schist, quartzite, marble, and granite (Farrell et al., 1999). These rocks may be divided into eight generic units (Farrell et al., 1999, figure 2-2) consisting of (i) Proterozoic clastics related to Neoproterozoic rifting; (ii) terrigenous detrital rocks of the Early Paleozoic miogeocline; (iii) Cambrian shallow-marine and carbonate platform strata; (iv) continental shelf-slope-rise sequences of the mature Paleozoic Cordillera passive margin; (v) Antler foredeep sediments; (vi) Early Tertiary basin deposits; primarily alluvial fan, fluvial, and lacustrine deposits; (vii) Miocene pyroclastic rocks of the Southern Nevada Volcanic Field; and (viii) Late Tertiary and Quaternary alluvial basin sediments with minor occurrences of basaltic volcanic rocks. As a consequence of these lithologic variations, differences in bulk porosity occur across the YMR. Primary porosities associated with these generic units may be modified further by diagenetic processes related to fluid flow, temperature, pressure, and organic activity. Modifications to these primary porosities also may occur in response to tectonic forces related to the structural setting of the region.

3.2 STRUCTURAL SETTING

Comprehensive discussions of the structural setting of the YMR are contained in Day et al. (1998a), Ferrill et al. (1998), and Farrell et al. (1999). As discussed by Fridrich et al. (1994), Bredehoeft (1997), Ferrill et al. (1998), and Farrell et al. (1999), the structural setting of the region plays an important role in the region's hydrogeology through its influence on the distribution of hydraulic conductivities and porosities. The following provides a brief summary of the structural setting of the region.

Rocks of late Proterozoic origin found in the Southern Great Basin have been deformed during several late Paleozoic and Mesozoic episodes of contractional deformation. This deformation produced several major faults and related structures in the YMR. The majority of faults at YM are either north-trending, normal faults or northwest-trending, dextral strike-slip faults. The larger faults in these two orientations bound the fault blocks that underlie much of the study area.

YM itself consists of a sequence of north-to-northeast-trending fault-bound ridges crossed by occasional northwest-trending, dextral strike-slip faults. Faults dip primarily to the west and separate blocks of gently east-dipping tuff strata. YM also contains numerous swarms of small northwest-trending faults that connect the large north-trending faults. In addition to major block-bounding and connected faults, minor faults or intra-block faults exist in the YMR. In some cases, these intra-block faults may

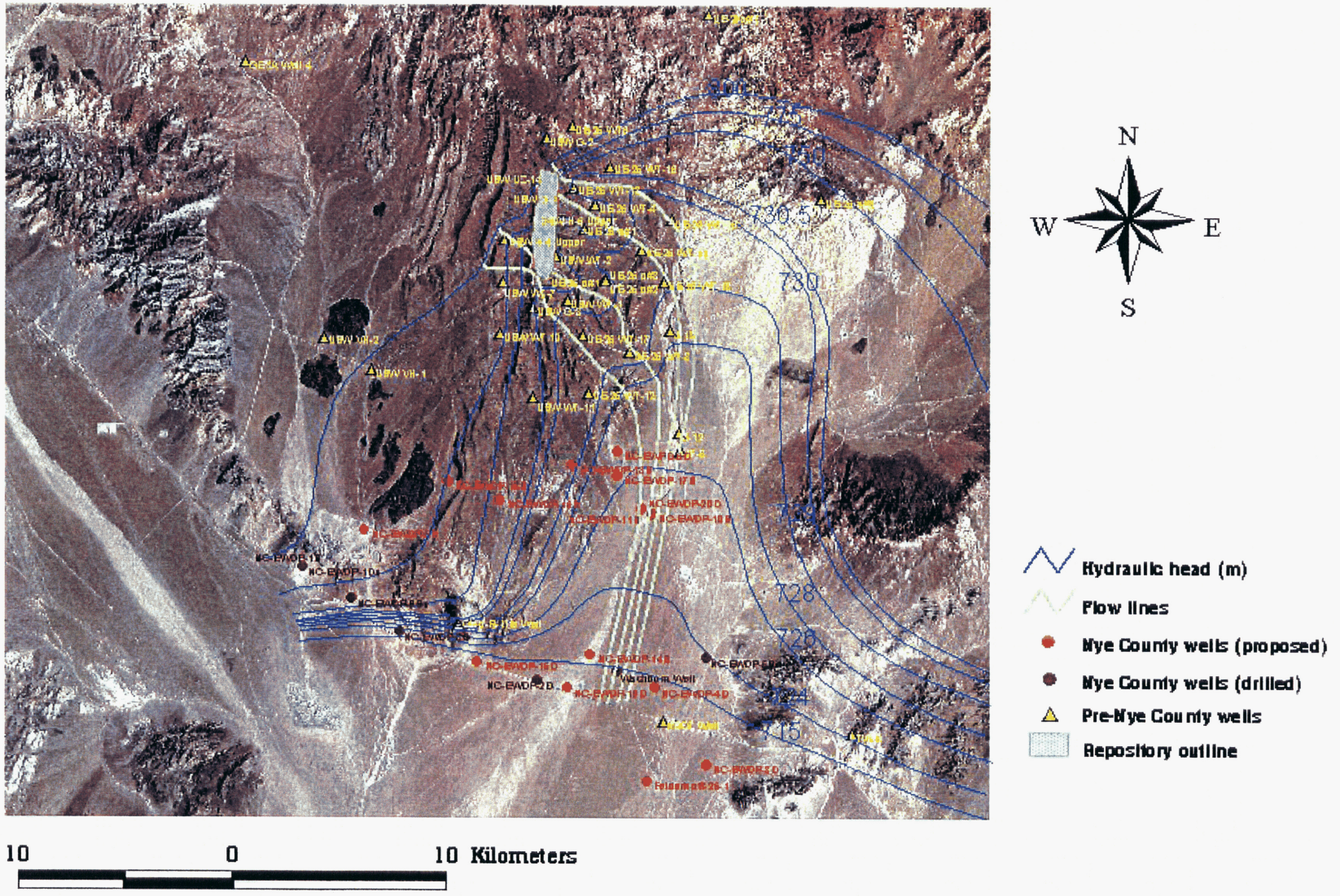

Figure 3-1. Site map of Yucca Mountain, Nevada, showing the water table, the repository, and the wells used to constrain the water table elevation

penetrate to depths of a few hundred meters from block-bounding faults (Day et al., 1998a). In addition to possibly enhancing groundwater flow, the presence of faults and fractures that result from tectonic processes contributes to the secondary porosity of the affected geologic units.

3.3 HYDROSTRATIGRAPHIC SETTING

The groundwater flow system in the YMR forms part of the larger Death Valley groundwater flow system which, in turn, is a subregion within the Great Basin regional aquifer system (Plume, 1996). Within the study area, the groundwater system can be described as a UZ, and four aquifer systems: one aquifer is located within the lower Paleozoic carbonate rocks, two are within the Miocene tuffs, and one is within the valley-fill or alluvial sediments. The latter aquifer appears only in the southern portion of the YMR and in the Amargosa Desert. Brief discussions of the various aquifer systems are presented in the following sections. It is important to note that although generic aquifer systems have been defined by some hydrogeologists (e.g., Luckey et al., 1996), there are locations within the YMR where units contained within aquifer systems may be unsaturated because of the complex geometries of the water table and the geologic units.

3.3.1 The Carbonate Aquifer

The carbonate aquifer beneath the YMR is part of the regional Death Valley hydrogeologic system. The aquifer consists of fractured and faulted Cambrian to Devonian carbonate rocks, overlying a lower confining unit that consists of Proterozoic to Cambrian clastic rocks, and underlies an upper confining unit that consists of Late Devonian to upper Mississippian clastic rocks.

For the YMR there is little information on the hydrogeologic properties of the carbonate aquifer (Winograd and Thordarson, 1975). What information there is has been obtained from one borehole, UE-25 p#1 (figure 3-1).

3.3.2 The Tuff Aquifers

Miocene volcanic deposits, primarily silicic tuffs, lying on an irregular surface, and up to 5 km thick in some places, obscure much of the underlying Precambrian and Proterozoic rocks of the YMR. The sources of the Miocene deposits are believed to be a series of Middle to Late Miocene calderas that compose the Southwestern Nevada Volcanic Field (Sawyer et al., 1994). The tuff sequence has been organized into the following stratigraphic groups; the Timber Mountain Group, the Paintbrush Group, the Calico Hills Formation, the Crater Flat Group, and a generic group composed of the Lithic Ridge and older tuffs (see table 3-1). The tuff units composing these groups are generally flat lying or in some instances moderately tilted in fault blocks bound by normal faults.

Hydrologically, the Miocene volcanics in the YMR may be divided into two aquifer systems and two confining systems based in part on porosity and associated permeability considerations. Luckey et al. (1996) described these units as the Upper and Lower Volcanic Aquifers (UVA and LVA, respectively) and the Upper and Lower Volcanic Confining units (UVCU and LVCU, respectively). It is important to note that in most instances lithologic units of the UVCU compose the UZ.

Table 3.1. Summary of the generalized stratigraphy and hydrostratigraphy of the Yucca Mountain Region (modified from Luckey et al., 1996)

Period	Stratigraphic Unit		Hydrostratigraphy
Quaternary	Valley-Fill (alluvium)		Valley-Fill (alluvial) Aquifer
Tertiary	Timber Mountain Group	Rainier Mesa Tuff	UZ ?????
	Paintbrush Group	Tiva Canyon Tuff	
		Yucca Mountain Tuff	
		Pah Canyon Tuff	
		Topopah Spring Tuff	Upper Volcanic Aquifer
	Calico Hills Formation		Upper Volcanic Confining Unit
	Wahmonie Formation		
	Crater Flat Group	Prow Pass Tuff	Lower Volcanic Aquifer
		Bullfrog Tuff	
		Tram Tuff	
	Lithic Ridge Tuff		Lower Volcanic Confining Aquifer
	Older tuffs, lavas, and breccias		
Early Permian and Pennsylvanian	Tippipah Limestone		?????
Missippian and Late Devonian	Eleana Formation		Upper Clastic Confining Unit
Cambrian to Devonian	Undifferentiated, primary carbonate rocks		Lower Carbonate Aquifer
Cambrian	Undifferentiated, primary clastic rocks		?????

The LVA includes most of the Prow Pass Tuff and the underlying Bullfrog and Tram units of the Crater Flat Group (Luckey et al., 1996). Where the upper part of the Prow Pass Tuff is relatively unfractured, it is considered part of the overlying confining unit (Luckey et al., 1996). The LVA underlies the majority of YM and its units are in most cases always within the SZ. In addition, the permeability of this aquifer is less than that of the UVA.

The LVCU consists of bedded tuffs, lava flows, and flow breccias beneath the Tram Tuff, in addition to the Lithic Ridge Tuff and the older flow (Luckey et al., 1996). In the vicinity of YM, this hydrostratigraphic unit has been encountered in boreholes USW G-1, USW G-2, USW G-3, USW H-1, J-13, and UE-25 p#1. It is argued that although some zones in the LVCU are fractured, the depth of burial of this unit results in fracture closure and, hence, poor transmission of water (Luckey et al., 1996). Additionally, calcite fracture fillings appear much more prevalent in the Lithic Ridge and Older Tuff units (Bish and Chipera, 1989) than in tuff units in the underlying Crater Flat Group.

The UVA is composed of variably welded ash flow tuffs and rhyolite lavas of the Topopah Spring Tuffs (TSw) (Luckey et al., 1996). This aquifer serves as the source of water for wells J-12 and J-13. Tectonic deformation, which produced an eastward dip of the volcanic units, resulted in the lower parts of the TSw being saturated in many regions around YM. However, beneath the proposed repository location, the entire TSw is unsaturated.

The UVCU consists of the unfractured part of the basal vitrophyre of the TSw, the bedded tuff beneath theTSw, the Calico Hills nonwelded Tuffs (vitric and zeolitic) (CHn), and the uppermost nonwelded part of the Prow Pass tuffs of the Crater Flat Group (Luckey et al., 1996). Although the unit is not considered an aquifer, it nevertheless is capable of producing water as demonstrated by Geldon (1993, figure 33). As such, the unit acts as a poor confining unit, thus allowing hydraulic communication between the UVA and the LVA (Winterle and La Femina, 1999). Beneath much of the southern part of YM, the upper part of this unit is above the SZ (cf., Fridrich et al., 1994; Luckey et al., 1996). In the remainder of the southern area, only the lower part of this unit is saturated. This is demonstrated by well USW WT-1, where only 8 percent of the unit thickness is saturated. Beneath YM, much of this unit is unsaturated.

3.3.3 The Valley-Fill Aquifer

Surface maps of Pliocene and Quaternary deposits in the Crater Flat and Fortymile Wash regions generally show "younging" of these deposits toward the south. This appears consistent with the interpretations of Ferrill et al. (1996) and Stamatakos et al. (1997) who suggest that the southern parts of these regions have undergone greater subsidence. The Quaternary deposits in these regions are commonly studded by Pliocene and Late Quaternary basaltic dikes and volcanoes that extend from the Amargosa Desert to Crater Flat.

Currently, little is known about the stratigraphy and hydrogeologic properties of the valley-fill deposits composing the alluvial aquifer. In the near future, however, more detailed information about the hydrogeologic properties of this unit will be obtained from the ongoing Nye County drilling program.

3.4 GROUNDWATER INFILTRATION, PERCOLATION, VELOCITIES, AND FLOWPATHS

Groundwater infiltration and deep percolation in the UZ at YM are controlled in part by the distribution of effective porosities. In general, for a given groundwater flux, the lower the effective porosity of the medium, the lower is its storage capacity and the greater the infiltration. Groundwater pore velocities and flow paths in the SZ in the YMR are controlled by the hydraulic gradient in the region, the spatial distribution of hydraulic conductivities, recharge, and effective porosities. Potentiometric maps developed for the YMR based on observed hydraulic head measurements in wells and other data appear to constrain the hydraulic gradient reasonably well and indicate flow from north of YM into the Amargosa Desert and beyond (Winterle et al., 2000; Winograd and Thordarson, 1975; Czarnecki and Waddell, 1984; Robison, 1984; Ervin et al., 1993, 1994). Because of uncertainties regarding the spatial distributions of hydraulic conductivities and porosities at the site, considerable uncertainty exists regarding groundwater flow paths and velocities. The spatial distribution of hydraulic conductivities in the YMR is discussed in Winterle et al. (2000) and is not reproduced here. Subsequent discussions in the report will focus on the spatial distribution of porosity and its potential impacts on groundwater flow velocities and mass transport.

3.5 SUMMARY

This chapter provided a brief overview of the geology and hydrogeology of the YMR. In general, there appears to be reasonable understanding of the complex distribution of geologic units within the YMR. Because of the complex distribution of geologic materials across the region, spatial distributions of porosity are complex. This complexity is further enhanced by ongoing geologic and hydrogeologic processes that continuously modify the primary porosities of the various geologic units both on the regional and local scale. A knowledge of the spatial distributions of these primary and secondary porosity features is essential for constraining groundwater flow velocities and mass transport in the YMR. In the following chapter, indepth discussions of the distribution of porosities in the various geologic units in the YMR are provided.

4 POROSITY DISTRIBUTIONS AT YUCCA MOUNTAIN

This chapter extends discussions begun in the previous chapter on porosity distributions along the groundwater flow path from the ground surface at YM to compliance points located to the south. To maintain consistency with the permeability report of Winterle et al. (2000), this chapter first discusses porosity distributions in the UZ at YM and later porosity distributions in the SZ along the proposed flow path. The chapter then concludes with a discussion of outstanding concerns regarding porosity along the flow path and possible approaches to resolving these.

For clarification, it is important to note that the UZ as discussed in this report refers primarily to the UZ beneath YM through which radionuclides may migrate, whereas the SZ is discussed from a more regional perspective. As a result, units that may occur in the UZ at YM may occur within the SZ at locations away from YM.

4.1 POROSITY DISTRIBUTIONS IN THE UNSATURATED ZONE

Discussions of porosity in this section are focused primarily on YM proper, that is, the area in which infiltration intercepting the repository occurs. The units considered pertinent to the ensuing discussions include the surficial alluvial units occurring on YM, the Tiva Canyon welded Tuff (TCw), the Paintbrush nonwelded Tuff (PTn), the TSw host unit for the repository, the CHn, the Prow Pass zeolitic and devitrified units, and the Bullfrog welded and nonwelded Tuffs. Away from YM, the TSw is located within the Upper Volcanic Aquifer, the CHn forms the Upper Volcanic Confining Unit, and the Prow Pass and Bullfrog units form the Lower Volcanic Confining Units (Luckey et al., 1996). As a result, porosities related to some of these units will be discussed in the SZ section of this report.

Literature on YM often describes two types of porosity, matrix and fracture. Matrix porosity essentially corresponds to primary or interstitial porosity discussed in chapter 2, while fracture porosity represents secondary porosity. In the YMR, fracture porosities are observed predominantly within the welded tuff units and may occur in response to tectonic and thermal processes.

The hydrostratigraphic layers in the UZ site-scale flow model (Civilian Radioactive Waste Management System, Management and Operating Contractor, 1998) are delineated based on measurements of porosity. Both matrix porosity and fracture density are correlated with degree of welding; hence, there is no further delineation of UZ hydrostratigraphic layers beyond that represented by porosity.

In the UZ at YM, the relationships between saturation and capillary pressure within the interconnected pores of the rock matrix and fracture networks play a vital role in determining the distribution of percolating fluxes throughout the mountain. Within this framework, porosity becomes important because it forms the basis of many pressure-saturation relationships often used to model this zone. As an example of the importance of porosity in the UZ, studies currently indicate that because average pore-sizes in the rock matrix are generally much smaller than fracture apertures, capillary suction may result in imbibition of water from fractures into rock. Imbibition of infiltration pulses continues until either the fracture runs dry or an equilibrium is reached. In this way, the interaction between the matrix and the fracture network has the potential to reduce groundwater fluxes along fractures, especially when the matrix moisture content is low.

Porosity generally is used as a surrogate variable for matrix K_{sat} (Flint, 1998; Rautman and McKenna, 1997) because (i) porosity has been measured on virtually all core samples, (ii) values of other hydraulic properties have not been determined for most core samples, and (iii) porosity appears fairly well correlated to hydraulic properties. Interestingly, a comparison of *in situ* water saturation and core-sample determined K_{sat} suggests that saturation may be a better predictor of K_{sat} than porosity (Nuclear Regulatory Commission, 1998). This correlation would be expected if the tuff matrix was near steady-state conditions in the thick UZ. For example, welded tuffs with appreciable lithophysae would have biased matrix porosity estimates. This is caused by the representative volume element for the lithophysal units being much larger than the core sample size.

4.1.1 Porosity Distributions in the Near-Surface

Infiltration into the subsurface is an important phenomenon at YM because it controls to varying degrees the amount of water available for deep percolation at the site, which in turn controls the volume of water that may contact waste packages and ultimately transport radionuclides to the water table. Shallow infiltration estimates are sensitive to porosity distributions within the near-surface. In general, matrix porosities of soils and bedrock are supported by measurements, whereas the porosity estimates associated with fractures in the near-surface are inferred.

Effective matrix porosities of soil have been estimated using weight relationships (Flint et al.,1996a, see appendix) from samples collected within the top 0.3 m in 8 of the 10 soil classes observed at YM. From the measured porosities, and measured grain size distributions, saturated hydraulic conductivities and moisture retention curves necessary for modeling groundwater flow and infiltration within the soil classes were predicted using mathematical formulae. The predicted estimates compared well with laboratory measurements of saturated hydraulic conductivity and moisture retention curves, performed on a limited number of the collected samples.

Field sampling of soils at YM is likely biased however, due to logistical problems such as the presence of boulders and cobbles, which limit the recovery of representative soil samples for laboratory analyses. The bias in sampling more-than-likely affects infiltration estimates because it generally leads to an overestimation of soil moisture capacity and therefore an underestimation of shallow infiltration. This leads to an underprediction of the deep percolation at the repository horizon.

The near-surface bedrock over the repository footprint is composed predominantly of moderate to densely welded TCw, although on the west flank, exposures of PTn and TSw occur. At the soil bedrock interface, cooling joints and tectonic fractures in the TCw either may be open completely or filled with soil/caliche. Matrix porosities for the near-surface TCw can be obtained from cores, however, total fracture porosity and porosities for filled fractures within this unit are all uncertain. The high degree of uncertainty associated with these parameters makes estimating groundwater infiltration difficult, and results of such estimates uncertain. This uncertainty is illustrated in the one-dimensional shallow infiltration models developed by NRC (Stothoff, 1999) and U.S. Geological Survey (USGS) (Flint et al., 1996b). In the USGS model, effective fracture and matrix porosities are combined in an explicit manner, with fracture porosity determined from borehole fracture frequency data and assumed fractions of area occupied by 2.5, 25, and 250 μm apertures. Calibrations based on neutron probe data led to the use of hydraulic conductivities estimated from filled fractures with apertures of 250 μm. A further assumption of the model is that soil layers can be treated as buckets that are filled sequentially, that is, the moisture capacity of the layer

(layer-capacity = effective-porosity × layer-thickness) must be exceeded before the water is transmitted to the next layer. In this model, water that moves below the root layer was considered shallow infiltration. The importance of effective porosity on this model is quite evident. In the NRC model, it is assumed that all water infiltrates through fractures that are either open, caliche-filled, or soil-filled, and that effective fracture porosities range 10^{-4}–10^{-2} for soil-filled fractures, and 10^{-5}–10^{-3} for caliche-filled fractures; the contribution of the matrix to shallow infiltration is assumed to be negligible. Shallow infiltration is simulated using a numerical solution of the Richards equation in the NRC model. Shallow infiltration estimates for the repository footprint for the NRC model are in the 6–12 mm/yr range (Nuclear Regulatory Commission, 1999), while for the USGS model the average is 4.6 mm/yr (Civilian Radioactive Waste Management System, Management and Operating Contractor, 1999a). The lower estimates of infiltration produced by the USGS model may be in part because of their overestimation of the effective fracture porosities.

4.1.2 Porosity Distributions from the Ground Surface to the Repository Horizon

The geologic units in the UZ located between the near-surface and the repository horizon include the TCw, the PTn, and the TSw. In most cases rocks within the UZ can be partitioned into those that primarily support fracture flow (e.g., TCw, and the TSw) and those that primarily support matrix flow (e.g., PTn). In the UZ, both fracture and matrix porosities strongly influence the distribution of flow.

Rates of deep percolation reaching the repository horizon and eventually the water table beneath YM depend on the hydraulic properties of the unsaturated rock units through which flow occurs. The fraction of water that flows in either the matrix or fracture is controlled by factors such as permeability, porosity, and capillary-saturation relationships of each geologic unit. As matrix porosities are generally much larger than fracture porosities, and pore sizes within the matrix are generally much smaller than fracture openings, most of the water in the UZ is held by capillary tension in the matrix, and as a result, matrix saturations are high and the fracture saturations are assumed to be low during ambient conditions. During ambient conditions, fractures present the dominant flow paths as exemplified by the welded volcanic tuffs at YM. As matrix permeabilities within the units of the UZ are sufficiently lower than the infiltration rate at YM, fractures are expected to provide the primary conduits or "fast flow paths" for infiltrating water to reach the repository level. The notion of flow in connected fractures causing rapid downward migration of infiltrating water is supported by geochemical data, in particular, the elevated levels of isotopes Cl^{-36} and Tc^{-99} observed at the repository level in the Exploratory Studies Facility (ESF) (Fabryka-Martin et al., 1996) and tritium in the CHn (Yang et al., 1996) beneath the repository.

The rapid flow of water through welded tuff units at YM is generally assumed to be caused by high fracture permeability. Contrasts between effective matrix porosity and fracture porosity may also impact flow within fractured rock units. For example, high matrix porosities, relative to fracture porosities, cause water to imbibe into the matrix during low matrix saturation. During conditions of high matrix saturation, however, less imbibition occurs, and, as a result, a greater portion of infiltration is available for fracture flow. The parameters that control the distribution of water between matrix and fractures are difficult to measure *in situ* and hence are highly uncertain.

The spatial distributions of matrix and fracture porosity at YM are important because they affect the spatial distributions of deep percolation reaching the repository horizon (see also the Spatial and Temporal Distribution of Flow Integrated Sub-Issue). To define the spatial distributions of matrix and fracture porosities within the geologic units of the UZ requires spatial measurements of porosity. At YM, techniques

designed to characterize these distributions mostly have relied on core measurements and pneumatic tests. Core measurements have been used primarily to analyze matrix porosities, whereas pneumatic measurements have been used to assess porosity in fractured zones. Because methods for measuring porosities from cores and pneumatic tests are extensively discussed in the appendix, no discussion of these methods is provided here. Instead, the following discussions will focus on the results of these analyses.

4.1.2.1 Effective Matrix Porosities in the Unsaturated Zone from the Ground Surface to the Repository Horizon

Numerous researchers have attempted laboratory analyses of rock core samples at YM (Anderson, 1981a,b; Rush et al., 1983; Anderson, 1984; Weeks and Wilson, 1984; Peters et al., 1984; Whitfield et al., 1984; Klavetter and Peters, 1987; Flint and Flint, 1990; Kume and Hammermeister, 1990; Anderson, 1991; Nelson et al., 1991; Loskot and Hammermeister, 1992; Loskot, 1993; Anderson, 1994; Rautman et al., 1995; Flint et al., 1996b). Recently, the USGS used 4,892 core samples from 23 shallow and 8 deep boreholes (figure 4-1; cf., Flint, 1998, table 1) in laboratory analyses to provide a detailed description of the rock properties, including effective porosity, at YM (Flint, 1998). On the basis of the laboratory tests performed, 31 hydrostratigraphic units were identified in the UZ. In the TCw, effective matrix porosities showed some variability that reflected the degree of vapor phase corrosion present. Effective matrix porosities for most of this unit were generally less than 9 percent except for several thin subunits near the base of this unit where effective matrix porosities exceeded 20 percent. Effective matrix porosities in the PTn unit showed less variability compared to the TCw and were generally greater than 40 percent. In the TSw, effective matrix porosities showed little variability and were generally less than 9 percent. In general, welded units tend to have the lowest porosities, while the nonwelded and bedded units tend to have the highest porosities. A summary of effective matrix porosities including the mean and standard deviation from each of the 31 hydrogeologic units is in table 4-1 (cf., Flint, 1998, table 7).

An important finding of this study was the recognition of transition zones with pronounced changes in porosities for short vertical distances. These porosity variations may reflect depositional and cooling histories, mineral alterations, and the presence of microfractures. As an example, at the top of the PTn, observed porosity variations, although rapid, were nevertheless continuous. At the base of the PTn, however, the porosity transition appears more discontinuous.

Observed porosity variations may also reflect the alteration of history of rocks at YM. For example, clay minerals, zeolites, opal, and calcite may form in place or may be deposited in pore throats or fracture apertures. In either case, their presence can alter porosity significantly. Other estimates of matrix porosity in the units above the watertable, in the vicinity of YM, have been presented by Anderson (1981a,b; 1984), Nelson et al. (1991), and Nelson (1996). Anderson (1981a,b; 1984) estimated effective matrix porosities for these units based on measurements performed on cores recovered from UE25a-1, UE25a-3, USW GU-3/G-3, and USW G-4. Effective matrix porosity profiles listed in these reports are qualitatively consistent with resistivity logs (Anderson, 1981a,b; 1984) and quantitatively consistent with unit effective matrix porosities listed in table 4-1. Nelson et al. (1991) reported on total matrix porosity estimates inferred from core measurements for the units above the watertable in the YMR. In most cases, the total porosity estimates contained in Nelson et al. (1991) showed general agreement with those given in Anderson (1981a,b; 1984). Total matrix porosities for the units above the watertable were also estimated from geophysical logs (in particular, density logs) by Nelson (1996). Comparisons of the core derived total porosities (Nelson et al., 1991) to logging derived total porosities for the UZ units, excluding the lithophysal zones of the TSw, generally showed total porosities derived from core analyses to be less than those derived from logging

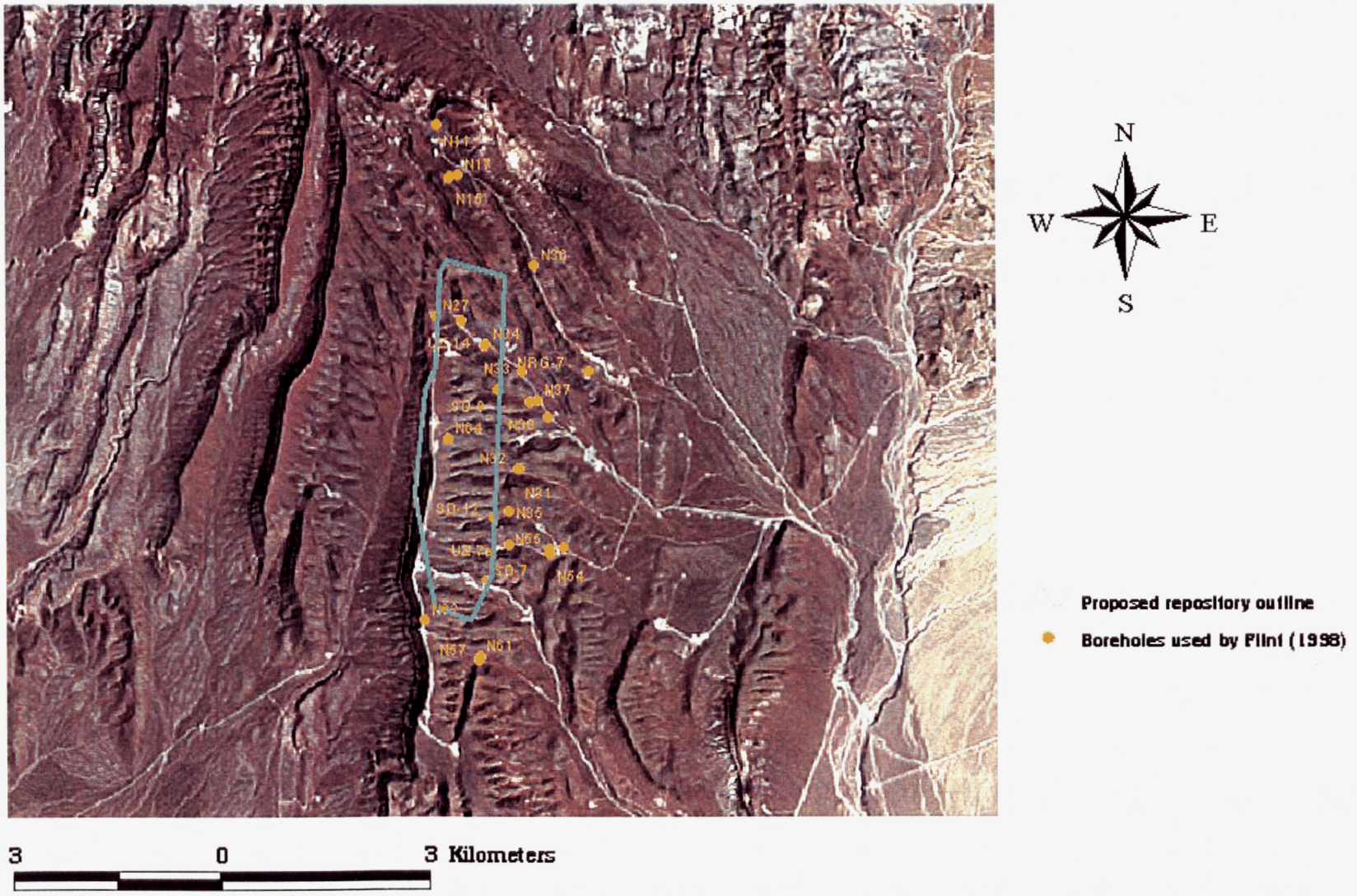

Figure 4-1. Map of Yucca Mountain, Nevada, showing the surface distribution of boreholes used to map the unsaturated zone

Table 4-1. Summary of effective porosity estimates from laboratory analyses of rock cores (Flint, 1998)

	Hydrogeologic Units	Porosity		
Major	Detailed	No. of samples	Mean	Standard deviation
Tiva Canyon Welded (TCw)	CCR	9	0.062	0.020
	CUC	101	0.253	0.060
	CUL	98	0.164	0.062
	CW	599	0.082	0.030
	CMW	90	0.203	0.054
	CNW*	101	0.387	0.070
Paintbrush Nonwelded (PTn)	BT4	33	0.439	0.123
	TPY	43	0.254	0.082
	BT3	85	0.411	0.079
	TPP	164	0.499	0.041
	BT2	171	0.489	0.105
Topopah Spring Welded (TSw)	TC	66	0.054	0.036
	TR	439	0.157	0.030
	TUL	455	0.154	0.031
	TMN	266	0.110	0.020
	TLL	453	0.130	0.031
	TM2	225	0.112	0.031
	TM1	102	0.094	0.019
	PV3	89	0.036	0.039
Calico Hills Nonwelded (CHn)	PV2	39	0.173	0.106
	BTla	36	0.288	0.072
	BT1	43	0.273	0.067
	CHV	69	0.345	0.034

Table 4-1. Summary of porosity estimates from laboratory analyses of rock cores (Flint, 1998) (cont'd)

	Hydrogeologic Units	Porosity		
	CHZ	293	0.331	0.039
	BT	69	0.266	0.041
	PP4	47	0.325	0.045
	PP3	166	0.303	0.043
	PP2	140	0.263	0.072
	PP1	245	0.280	0.053
Crater Flat (CFu)	BF3	86	0.115	0.040
	BF2	65	0.259	0.084
*Part of CNW is classified as PTn in Flint (1998)				

analyses. These differences may result from underrepresentation of lithophysae in the cores used in the analyses, and approximations present in the reduction of the logging data (Nelson, 1996).

Comparisons of measured physical and hydraulic properties for the vitric units, such as the moisture retention parameter, α, and the saturated hydraulic conductivity, to effective porosity demonstrate correlation (Flint, 1998, figure 14). This correlation is important for estimating values for these parameters at locations where only effective porosities are available. Unfortunately, similar correlations do not appear to exist for other geologic units at the site (Flint, 1998).

4.1.2.2 Effective Fracture and Fault Porosities in the Unsaturated Zone from the Ground Surface to the Repository Horizon

Groundwater flow and transport properties in the UZ have also been determined using *in situ* methods. One approach applied at YM involves the use of pneumatic injection and gaseous tracer-tests. Discussions of the pneumatic method are given in the appendix, section 3.2.4, while discussions of the gaseous tracer-test method are provided in LeCain (1998). In particular, these methods have been applied extensively to estimate flow and transport properties along fault and fracture zones, where recovery of undisturbed cores is virtually impossible. In general, measurement scales associated with these methods are significantly greater than those associated with laboratory and core-scale measurements.

Cross-hole pneumatic injection tests were conducted by USGS staff in boreholes located in the Bow Ridge Fault Alcove (BRFA) (figure 4-2; cf., LeCain, 1998) to test the pneumatic properties of the fault zone. Details of the tests are outlined in LeCain (1998) and are not reproduced here. The two horizontal, parallel boreholes (HPF#1 and HPF#2) used in the test were located 3 m apart and penetrated the crystal-poor middle lithophysal zone of the TCw, the Bow Ridge Fault zone, and the pre-Rainier Mesa Tuff. Values of effective

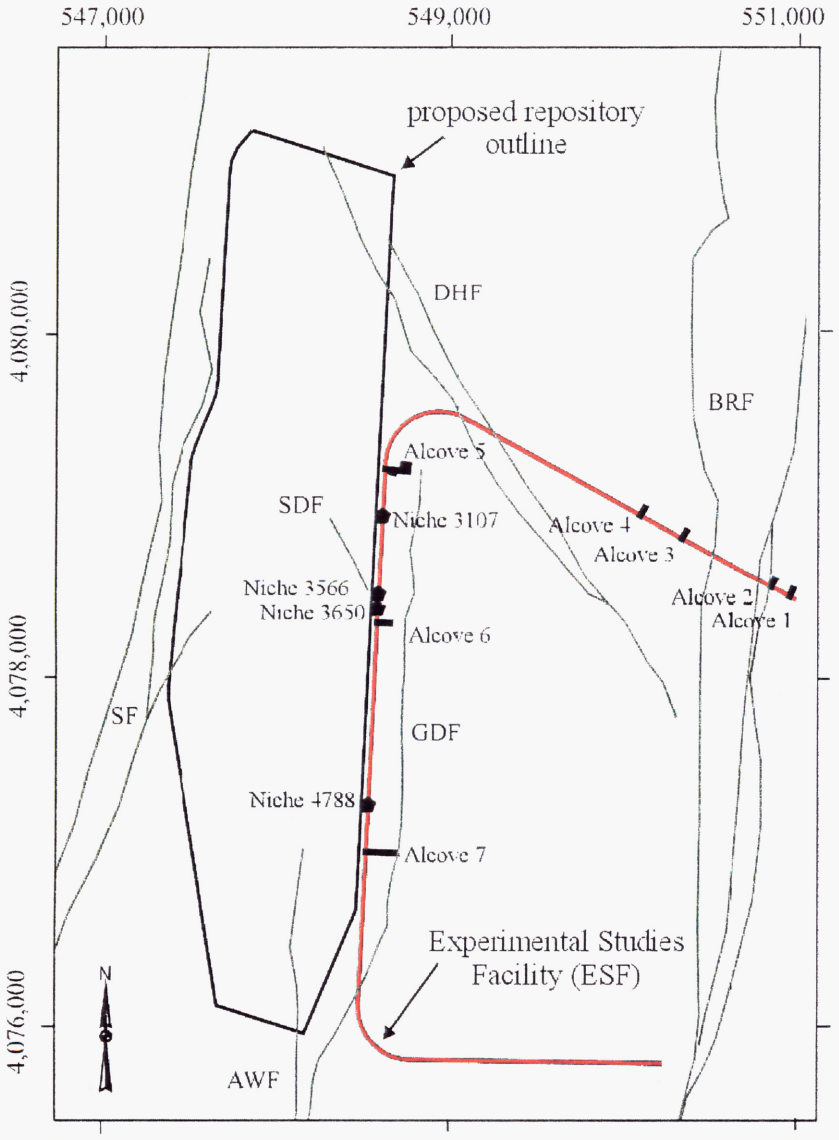

BRF : Bow Ridge fault
GDF : Ghost Dance fault
AWF : Antler Wash fault
SF : Solitario Canyon fault
DHF : Drillhole Wash fault
SDF : Sun Dance fault

Figure 4-2. Distribution of alcoves in the Exploratory Studies Facility

porosity reported by LeCain (1998) based on these tests were 0.13 and 0.20 for the Bow Ridge fault zone. Effective matrix porosities for the pre-Rainier Mesa Tuff was 0.27. In addition to the pneumatic tests, LeCain (1998) evaluated effective fault zone porosities at the site with convergent gaseous tracer-tests using sulfur hexafluoride (SF_6) (see LeCain, 1998, for technical details). Effective fault zone porosity estimates resulting from the tracer-tests (0.48–0.52 and 0.22–0.24) exceeded those values obtained from cross-hole pneumatic injection tests. Possible reasons for the discrepancies cited in LeCain (1998) include increased tortuosity and tracer adsorption. A summary of results from the tracer-tests is provided in table 4-2.

Cross-hole pneumatic injection tests were also conducted across the northern part of the Ghost Dance Fault located in the Northern Ghost Dance Fault Alcove (NGDFA) (LeCain et al., 1999). Data obtained from the tests were interpreted to indicate three zones, with differing pneumatic properties, associated with the footwall, fault zone, and hangingwall of the fault. Effective porosities (matrix plus fracture) for the footwall and the hangingwall were approximately 0.04, whereas the effective porosity of the fault zone was observed to be approximately three times larger (0.13). Convergent gaseous tracer-tests were conducted at the same location using sulfur hexafluoride (SF_6) and helium (He) as the tracers. Interpreted results from the tracer-tests indicated the method was unable to identify differences in effective porosity between the matrix (0.13) and the fault zone (0.14). The observed porosity discrepancies between the two methods may result from varying test conditions and interpretation errors.

It is interesting to note that the minimum effective porosities (1×10^{-3}) observed in NGDFA are generally 1–2 orders of magnitude greater than fracture porosities used to calibrate the UZ flow model developed for the VA (Civilian Radioactive Waste Management System, Management and Operating Contractor, 1998). This discrepancy may be in part because of two factors: (i) fracture apertures in the rock in which the pneumatic tests were performed are not representative of fracture apertures in the UZ and (ii) there were limitations in the approach used by Sonnenthal et al. (1997) to determine fracture porosities for the UZ flow model. While evaluation of the former requires additional data, the latter has been addressed by Winterle et al. (1999a) who stated that mixing fracture frequency data corrected for geometric orientation with uncorrected data in the DOE approach could be a potential source of error. Another source of error could be the 1-m length cutoff for fracture characterization in the ESF; the connectivity threshold for the fracture network may be significantly lower than the measurement length cutoff.

Limitations associated with the design of pneumatic tests and subsequent data interpretation have been illustrated and discussed by Illman et al. (1998). In their work, cross-hole pneumatic injection tests were conducted at an analog site to YM in central Arizona consisting of welded tuffs near the soil surface. Air filled porosity values were obtained by means of type-curve interpretations of pressure records derived from monitoring intervals located for distances 2.0–23.2 m. The air filled porosities reported by Illman and Newman[1] from a cross-hole test range between 2.9×10^{-5} (0.003 percent) and 7.2×10^{-2} (7.2 percent), with an arithmetic mean of 1.7×10^{-2} (1.7 percent), variance of 3.9×10^{-4}, and coefficient of variation equal to 1.2. It was found through their analyses that estimates of air-filled porosities varied strongly with location and direction when the pressure data from each monitoring interval were interpreted separately and the rocktreated as an isotropic, homogeneous continuum. On the other hand, when the same cross-hole pneumatic

[1] Illman, W.A., and S.P. Neuman. Type-curve interpretation of a cross-hole pneumatic test in unsaturated fractured tuff. *Water Resources Research*. Submitted for publication. 2000.

Table 4-2. Results from cross-hole tracer-tests in Bow Ridge Fault Alcove (adapted from LeCain, 1998)

Test number	Pumped interval in HPF#1	Release interval in HPF#2	First arrival [min]	Peak arrival [min]	Tracer velocity [$\times 10^{-4}$ m/s]	Darcy velocity [$\times 10^{-4}$ m/s]	Effective porosity
2	Bow Ridge fault zone	Bow Ridge fault zone	16	80	6.5	3.1–3.4	0.48–0.52
3	Bow Ridge fault zone	Bow Ridge fault zone	16	36	14.4	3.1–3.4	0.22–0.24

test data were interpreted by means of a numerical inverse approach, which resolves heterogeneities down to a scale of 1 m^2 (Vesselinov and Neuman, 2000), the estimated porosities are much smaller than those obtained via methods that treat the rock as uniform. This finding suggests that a reevaluation of the pneumatic test data collected at the NGDFA, and at all other test areas, using more robust techniques may be required to resolve the discrepancy between computed effective porosity and that used in the UZ flow model developed for the VA (Civilian Radioactive Waste Management System, Management and Operating Contractor, 1998).

The Lawrence Berkeley National Laboratory (LBNL) pneumatic testing program (Tsang et al., 1996) in connection with the single-heater experiments and niche studies (Wang et al., 1997) yielded numerous single- and cross-hole pneumatic pressure data in the ESF. Those data have not been interpreted adequately to yield estimates of porosity at the time this report was written. The simultaneous inversion of cross-hole pneumatic data in Huang et al. (1999) assumes an effective porosity throughout the modeled region. The transient interpretation of the cross-hole pneumatic pressure data using analytically derived type-curves or numerical inverse interpretation may yield information on porosity and its spatial distribution in the future. It appears that more work may be required in interpreting pneumatic test data from YM.

Finally, fracture porosity estimates based on field hydraulic and pneumatic tests are lacking for the lower lithophysical unit of the TSw in which the majority of the repository will be located. Ongoing field tests in the Cross-Drift should provide some of this additional information.

4.1.2.3 Subsurface Monitoring of Barometric Pressure Fluctuations

Measurements of bulk diffusivity in the UZ (e.g., Rousseau et al., 1997a), when taken alone, are generally of little use for predicting flow rates and the distribution of flow in unsaturated media. Monitoring of ambient pressure fluctuations, however, may provide important insight into bulk, site-scale estimates of intrinsic diffusivity in the UZ.

---

[2] Chen, G., W.A. Illman, D.L. Thompson, V.V. Vesselinov, and S.P. Neuman. Geostatistical, Type-Curve, and Inverse Analyses of Pneumatic Injection Tests in Unsaturated Fractured Tuffs at the Apache Leap Research Site Near Superior, Arizona. *Dynamics of Fluids in Fractured Rocks—Concepts and Recent Advances, in Honor of Paul A. Witherspoon's 80th Birthday*. In press. 2000.

USGS and LBNL staffs independently have simulated observed barometric fluctuations across several lithologic units with varying degrees of success. In particular, the results of these simulations indicate that because of the apparent lack of barometric signal attenuation and lag through the TCw and TSw Tuffs, the effective matrix porosities of these units is relatively low, and fracture flow dominates in these units. Contrary to this observation, significant barometric signal lag and attenuation occurred across the PTn unit indicating high effective matrix porosities and suggesting greater flow within the matrix. Interestingly, the degree of signal lag and attenuation (Rousseau et al., 1997b; Patterson et al., 1996; Ahlers et al., 1999) may reflect to some degree spatial variations in matrix saturation as well as the presence of fractures. Spatial variations in the thickness of the unit also may be responsible partially for the observed spatial variations in signal lag and attenuation.

4.1.2.4 Effective Porosities of the Geologic Units Surrounding the Repository During the Postclosure Period

Prior to the emplacement of HLW, the effective fracture and matrix porosities of the rock in the vicinity of the repository are expected to be similar to that of the host geologic unit. During the postclosure period, heat produced by the wastes will significantly elevate the temperature of the adjacent rock. This heating is expected to result in refluxing of moisture contained in the pores and fractures of the surrounding rock mass. Whether the elevated temperatures and associated refluxing will lead to geochemical alteration of the surrounding rock is not well understood. It is possible, however, that should geochemical alteration take place, changes in effective matrix and fracture porosities may occur through such processes as mineral dissolution, transport, and precipitation. Expansion of the rock mass surrounding the repository owing to the elevated temperature is also a possibility. Should this happen, changes in effective fracture, and perhaps matrix, porosity may also occur. Further investigations of these processes may be required to assess their impacts on effective porosity and repository performance.

In addition, it is expected that during the postclosure period, deformation of the repository geometry will take place through mechanical loading and associated stresses. Although the full extent of this deformation is not completely understood, it is possible that it may lead to the generation of new fractures and the opening and closure of existing fractures. Should this happen, changes in the effective fracture porosity of the rock around the repository may occur. Further investigations of these processes may be required to assess their impacts on effective porosity and repository performance.

4.1.3 Porosity Distributions from the Repository Horizon to the Water Table

It is generally difficult to define the units between the repository horizon and the water table because of the complex geometries of the water table and the unit layers. These geometric relationships result in units, such as the Prow Pass and Bullfrog Tuff units, lying above the water table at some locations and below the water table in other locations. Away from YM these units are generally grouped in the SZ (e.g., Luckey et al., 1996) and are discussed in the SZ section of this report. Analyses by Flint (1998) indicates that at YM, the Prow Pass Tuff is composed of both zeolitic and devitrified tuffs with effective matrix porosities ranging 20–40 percent. The Bullfrog Tuff is composed of primarily welded and nonwelded tuffs, with effective porosities for the welded tuffs on the order of 20 percent and that for the nonwelded units greater than 60 percent.

The CHn, which overlies the Prow Pass Tuff is entirely within the UZ at YM. Should the engineered system at the repository fail, it is expected that radionuclides will migrate through this unit. Therefore, both the hydraulic and geochemical properties of this unit are important for repository performance. Because the hydraulic and geochemical processes that affect groundwater flow and radionuclide transport are influenced to varying degrees by effective porosity, an understanding of the distribution of this property in the CHn is essential.

Because the porosities of these subunits are quite similar, porosity differences alone cannot be used as a basis for distinguishing between them. Instead, the units are differentiated based on two criteria, residual saturations and total porosity. Using this approach, the division between the two subunits is defined based on a 5 percent difference in porosities measured during (i) elevated relative humidity drying conditions, defined as 65 percent relative humidity at 60°C; and (ii) standard oven drying conditions, defined as 105°C at ambient relative humidity (Flint, 1998). That is, if the difference in estimated porosity for a sample is greater than 5 percent when both approaches are employed, the sample is classified as zeolitic.

The current conceptual model for flow through the nonwelded units below the repository predominantly has matrix flow through the vitric units and fracture flow or lateral diversion around the zeolitic units. While little sorption of radionuclides occurs during fracture flow or diversion around the zeolite units, there is a large potential for sorption during matrix flow through the nonwelded vitric units. As a result, the delineation of vitric and zeolitic units in the CHn is important for repository performance (Winterle et al., 1999b).

4.1.3.1 Estimates of Matrix Porosity in the Calico Hills Formation

Although the CHn is generally considered important to repository performance, few boreholes intersect this unit. On the basis of the limited data that exist for this unit, the mean porosity estimated from laboratory analyses of rock cores from the vitric unit is approximately 0.35. This value lies in the 0.3–0.37 range estimated for the porosities of the zeolitic units (Flint, 1998).

4.1.3.2 Estimates of Fracture Porosity in the Calico Hills Formation

Fracture porosities for the CHn have been estimated using approximated apertures and fracture frequency. The estimated fracture porosities used were based on the assumption of constant aperture throughout the length of the fracture, hence, effective fracture porosity is computed as the product of the fracture aperture and the number of fractures observed. Fracture porosities estimated using this approach range between 6.9×10^{-4} and 8.9×10^{-4} for the vitric zones, while estimates for the zeolitized zones range between 1.7×10^{-4} and 4.3×10^{-4} (Civilian Radioactive Waste Management System, Management and Operating Contractor, 1999b). Limited data are available to support these estimates, so it may be possible to use the PTn as an analog because both zones are nonwelded, and the PTn has more boreholes and surface outcrop data.

4.2 POROSITY IN THE SATURATED VOLCANIC TUFF AQUIFER

Estimates of groundwater pore velocities in the saturated volcanic tuffs beneath YM are required to assess the efficacy of these geologic formations as natural barriers to radionuclide migration. For steady, uniform flow in homogeneous porous media, groundwater pore velocity is estimated simply by dividing

groundwater flux by the effective porosity of the medium. Unfortunately, estimation of effective porosity in the tuff aquifer is complicated by the heterogeneous nature of the flow system, as evidenced by numerous borehole-flow surveys that indicate transmissive intervals are widely spaced, occurring predominantly within zones of interconnected fractures that dissect partially to densely welded rocks of low matrix permeabilities (e.g., Geldon, 1993; Luckey et al., 1996). In such strongly heterogeneous systems, effective porosities, and, hence, groundwater velocities, are spatially variable.

In contaminant transport calculations, the fact that some groundwater may travel faster or slower is often lumped into a hydrodynamic dispersion term of the advection-dispersion equation. In the fractured-tuff aquifer beneath YM, however, the strong permeability contrast between the rock matrix and fracture networks causes the major portion of flow in the tuff aquifer to occur in the small fraction of the aquifer pore space that comprises interconnected fractures. As such, for of discussing flow in the tuff aquifer, it is necessary to distinguish between effective flow porosity and matrix porosity. Effective flow porosity consists of interconnected networks of permeable fractures, faults, bedding planes, and high-permeability matrix pathways. The terms "effective flow porosity" and "fracture porosity" are used interchangeably in this section. Matrix porosity is generally associated with the pore space of low-permeability rock matrix and dead-end, low-permeability, and isolated fractures.

In both DOE and NRC PA models, the tuff aquifer is treated as a dual-porosity system for radionuclide transport modeling. Dual-porosity transport models treat the fracture and matrix porosities as two interacting continua and are based on the assumptions that (i) all advective transport occurs in the fracture continuum, (ii) the distribution of pore velocities within the fracture continuum can be addressed in transport calculations using a hydrodynamic dispersion coefficient, and (iii) dissolved solutes enter and leave the matrix continuum via diffusive exchange with the fracture continuum.

4.2.1 Matrix Porosity

Rock-matrix porosities of the geologic formations in the volcanic tuff aquifers and confining layers have been exhaustively studied on the scale of rock core samples (e.g., Peters et al., 1984; Anderson, 1991, 1994; Flint, 1998). The matrix porosities reported by Flint (1998) are broadly consistent with the earlier studies and provide an excellent basis for estimating flow and transport model parameters. Additionally, the large number of samples analyzed by Flint (1998) provides an understanding of spatial variability within stratigraphic units. With few exceptions, matrix porosities estimated for the stratigraphic units of the upper and lower volcanic aquifers range from about 0.1 to 0.3.

Because flow in the upper and lower volcanic aquifers at YM is conservatively assumed to occur entirely in fracture networks, knowledge of matrix porosity in the SZ is important only insofar as it affects matrix diffusion in contaminant transport calculations. Matrix diffusion is defined as the migration of solutes from flowing fractures into the more or less stagnant pore space within the low-permeability rock matrix and dead-end fractures. Hence, greater matrix porosity provides increased immobile storage capacity for dissolved contaminants. PA sensitivity analyses demonstrate that matrix diffusion is likely to provide only a modest benefit for repository performance when a 20-km compliance boundary is selected (Winterle et al, 1999b). Because matrix porosity is only one of several factors that affect matrix diffusion, and because matrix diffusion is only marginally important to repository performance, it should be sufficient for PA calculations to simply assume a constant matrix porosity value of about 0.2 for saturated volcanic tuffs. It must be noted, however, that if flowing fracture zones in the saturated tuffs are spaced far apart and advective velocities are

high, then diffusing solutes only partially may penetrate the rock matrix during the time scale for advective transport through the fractured tuffs. As such, depending on the transport model selected, effective immobile porosities may be somewhat less than the total matrix porosity. For example, in the TPA code used by NRC (Mohanty and McCartin, 1998), the rate of matrix diffusion is assumed proportional to the difference between fracture (mobile) solute concentrations and the volume-averaged matrix (immobile) solute concentrations. Because matrix solute concentrations are volume averaged in this type of model, only the fraction of matrix that has been permeated by diffusing solutes should be considered. For this reason, the latest revision of the NRC TPA code (in preparation) contains a new parameter—the Immobile Porosity Penetration Fraction—to account for limited matrix penetration by mobile solutes.[3]

4.2.2 Effective Flow Porosity

Estimates of effective flow porosity for the volcanic tuff aquifer vary by orders of magnitude. L. Gelhar of the SZ Expert Elicitation Panel suggested that a value of 0.001 seems plausible, but effective porosities could range from 10^{-5} to 0.01 (Geomatrix Consultants, Inc., 1998). Effective porosity estimates from other panel members generally fall within this range. For example, S. Neuman suggested the spatial distribution of effective porosity might be lognormally distributed with a geometric mean and 10^{th} and 90^{th} percentiles of 0.01, 0.001, and 0.1, respectively.

Estimates obtained from interpretation of tracer-tests at the C-Holes Complex tend to be relatively high. An effective porosity estimate of 0.086, for example, was obtained by USGS from interpretation of an iodide tracer-test in the Bullfrog Tuff by Geldon et al. (1997), using the analytical method of Moench (1995). An independent analysis of the iodide tracer-test by CNWRA staff using the same approach yielded a value of 0.028, which, although somewhat lower, is of similar magnitude. The lower value obtained by CNWRA staff is mainly the result of differing assumptions regarding the thickness of the transmissive interval. Interpretation of a multiple tracer-test by Los Alamos National Laboratory (LANL) staff yielded a range of 0.0027–0.25 for effective flow porosity in the Bullfrog Tuff (Reimus et al., 1998). Additional tracer-tests have been conducted in the Prow Pass Tuff interval at the C-Holes Complex, but interpretations of these data have not been made available yet.

Winterle and La Femina (1999) indicated that a number of the assumptions used in the USGS and LANL interpretation methods could result in significant overestimation of effective flow porosity. The authors concluded that the nominal and upper bound estimates of effective porosity from the C-Holes Complex tracer-tests in the Bullfrog Tuff are unrealistically high because the interpretation methods neglect three important factors: (i) the background hydraulic gradient, (ii) the fracture network tortuosity, and (iii) the assumption that flow is confined within a horizontally continuous test interval. Neglect of the background hydraulic gradient could bias significantly porosity estimates toward higher values when the direction of interwell tracer circulation is counter to the prevailing hydraulic gradient. Neglect of fracture tortuosity and vertical components of flow outside the test interval would also bias porosity estimates toward higher values, though perhaps to a lesser extent.

Additional insight into effective flow porosity may be gained by examining the observed spacings between production zones in wells that tap the volcanic tuff aquifer. The best available sources of such data for this topic are the flow-meter surveys reported for several boreholes near YM. An analysis of transmissive

[3] McCartin, T. Personal Communication (February 24) to J. Winterle. 2000.

interval spacing was conducted by researchers at Sandia National Laboratories (SNL). Preliminary results of their analysis, which included corrections for borehole and fracture orientations, indicate the spacing between flowing fracture zones in the volcanic tuffs is lognormally distributed with mean, and standard deviation $\log_{10}$ values of 1.3 and 0.43 (Civilian Radioactive Waste Management System, Management and Operating Contractor, 1999c). This translates to an typical transmissive-zone spacing of about 20 m, with a range of about 2–200 m. This SNL analysis compares favorably with an analysis by Winterle and Murphy (1999), who inferred effective flow zone spacings in the tuff aquifer on the order of tens to hundreds of meters, based on distributions of calcite mineralization in the SZ and calculated calcite dissolution rates. The two orders of magnitude range of observed transmissive interval spacings indicate that the spatial distribution of effective porosity may be quite heterogenous in the upper and lower volcanic tuff aquifers.

Using the preceding estimates of transmissive interval spacing and available aquifer transmissivity data, a crude estimate of bulk effective porosity can be obtained using the Cubic Law (e.g., Witherspoon et al., 1980). The Cubic Law relates the bulk permeability (k) in a system of parallel fractures to the effective fracture aperture (b) and the effective distance between fractures (L) according to the equation

$$k = \frac{b^3}{12L} \tag{4-1}$$

Rearranging to solve for b produces

$$b = \sqrt[3]{12kL} \tag{4-2}$$

East of YM, transmissivities in the tuff aquifer are on the order of 1,000 m^2/d at scales from 0.1 to several kilometer (e.g., Geldon et al., 1997; Winterle and La Femina, 1999). Using an estimated vertical thickness of 400 m for the lower volcanic aquifer and a water temperature of 30 °C, this translates into bulk aquifer permeability on the order of 3×10^{-12} m^2. Substituting this value into Eq. (4-1) yields an effective fracture aperture on the order of 1 mm for flowing fractures spaced 20 m apart. Effective porosity is estimated from the ratio b/L, yielding an effective porosity on the order of 5×10^{-5}.

For several reasons, the effective porosity estimate from the preceding Cubic-Law analysis can be considered an overly conservative lower bound. First, transmissive zones in boreholes are not realistically represented by the concept of a single 1-mm fracture every 20 m. Many, if not most, transmissive intervals contain zones of intense fracturing (e.g., Geldon, 1996). To produce the same permeability as a single 1-mm fracture, it would take, not 10, but 100 fractures with a 0.1-mm aperture. This is true because the permeability of a single fracture is proportional to the square of the aperture. If we repeat the preceding Cubic-Law analysis assuming zones of 100 closely spaced 0.1-mm fractures with a 20-m spacing, the effective porosity estimate increases tenfold. A second factor to consider is that the Cubic-Law model does not account for flow path tortuosity. Tortuous flow paths would require greater individual fracture permeabilities, hence, wider fracture apertures, to produce the same bulk aquifer permeability as a system of parallel planar fractures. Third, the coefficient value of 12 in Eq. (4-2) is applicable to smooth-walled fractures. For rough-walled natural fractures, this coefficient should be somewhat greater (Witherspoon et al., 1980), resulting in a higher effective porosity estimate. A fourth consideration is that the preceding analyses consider only major transmissive intervals identified in borehole-flow surveys to estimate effective fracture spacing. Minor

transmissive zones that may not be revealed in borehole flow surveys could make up additional flow porosity that is not considered.

Based on the previous discussion, a value of 0.001would be a reasonable lower bounding value for effective flow porosity when used in PA models to represent aquifer-scale flow through the lower volcanic tuff aquifer down-gradient from YM. Based on opinions expressed by the expert panel and results obtained from tracer-tests at the C-Holes Complex, a value of 0.01 is a reasonably conservative upper bound for effective flow porosity in the tuff aquifer.

4.3 POROSITY OF THE SATURATED VALLEY-FILL AQUIFER

Estimates of groundwater velocities in the saturated valley-fill units located south of YM are required to assess the efficacy of these units as natural barriers to radionuclide migration. Current consensus between DOE and NRC is that most of the attenuation in radionuclide concentration along the flow path will occur in the valley-fill units because of (i) the lower groundwater velocities (compared to the tuff units) expected due to the anticipated higher porosities, (ii) the associated high mineral surface area to volume ratio within these units, and (iii) the mineral compositions of the units. Winterle et al. (2000) also suggest that matrix diffusion processes may contribute to further attenuation of radionuclide concentrations in the valley-fill units. Winterle et al. (2000) postulate that radionuclides can diffuse into pore spaces contained in large cobbles or clay lenses in which low permeability results in minimal advective mass transport.

Currently, there is limited data on the hydraulic properties of the valley-fill units. As a result, both the DOE and the NRC currently assume in PA models that the hydraulic properties of these units are homogeneous. NRC TPA Version 3.2 code currently assumes that effective porosity follows a uniform distribution between 0.1 and 0.15. This range is based on crude estimates of specific yield provided by Walker and Eakin (1963). It should be noted that Walker and Eakin's values are not based on data from the valley-fill sediments south of YM, but are instead based on estimates from other sites that they considered reasonable analogs. Total porosity measurements performed in near-surface valley-fill sediments, composed of varying quantities of sands and silts, located at the low-level radioactive waste site near Beatty, Nevada, range between 0.25 and 0.45 (Fischer, 1992). These measurements suggest values of effective porosity that initially may appear to exceed measurements of Walker and Eakin (1963). Because these sediments have undergone little compaction, their porosities may not be representative of porosities in the valley-fill deposits below the water table south of YM. DOE currently assumes that effective porosity can be modeled as a truncated normal distribution with mean 0.25 and standard deviation 0.075 (Civilian Radioactive Waste Management System, Management and Operating Contractor, 1998). The higher values of effective porosity currently used by the DOE result in less conservatism than is present in the NRC model.

Although DOE and NRC currently treat the valley-fill deposits as homogeneous, data from geophysical surveys (e.g., Farrell et al., 2000; Oatfield and Czarnecki, 1991), geophysical well logs (neutron, caliper, and resistivity in particular; see Nye County Early Warning Drilling Program, Phase 1–FY1999, Data Package), and drill cuttings indicate these deposits are composed of spatially varying thicknesses of sands, gravels, silts, clays, and cobbles. As a result, the porosity of the valley-fill unit can be expected to show considerable spatially variability. It is hoped that properly calibrated and standardized geophysical logs for the Nye County wells will yield estimates of the effective and total porosities of the valley-fill units. Planning also is currently underway to construct an Alluvial Testing Complex, which will consist of several wells, optimally located and spaced for conducting cross-hole hydraulic and tracer testing. When available, porosity

estimates derived from both the tracer-tests and the geophysical logging will be used in groundwater flow and mass transport simulations, as well as to provide input distributions or bounding values for PA simulations.

4.4 SUMMARY

This chapter presented a review of porosity variations in the major geologic units at YM and the surrounding region that lie along the groundwater flow and potential radionuclide migration pathways extending from the ground surface above the repository to compliance points to the south. In general, the effective porosity varies across, as well as within, geologic units. In addition, effective porosities at the site may be grouped into effective matrix porosities and effective fracture porosities.

Effective matrix and fracture porosities in the near-surface environment affect the distribution and volume of infiltration fluxes at YM. Current methods for estimating effective matrix porosities for soils and rock are robust, however, concerns exist with regard to possible biases in soil sampling procedures that may upwardly bias estimates of bulk effective matrix porosity and soil moisture capacity at the surface of YM. Overestimation of soil moisture capacity would lead to underestimation of shallow infiltration and deep percolation. Effective fracture porosity distributions in the near-surface bedrock also influence the distribution and volume of infiltration fluxes. Uncertainties with regard to estimates of this parameter can result in uncertainties in estimates of infiltration fluxes.

For the tuff units making up the UZ, a database consisting of over 4,000 effective matrix porosity values, estimated from careful measurements on drilling cores, has been compiled. The database reveals a correlation between effective matrix porosities and the degree of welding present in the units. Nonwelded rock units, for example, possessed the highest matrix porosities (on average above 40 percent for the PTn, and 30 percent for the CHn), while welded rocks generally showed lower effective matrix porosities (on average less than 9 percent for the TCw, and 10 percent for the TSw). Some degree of bias may also exist because of the limited number of samples collected for each unit (e.g., only two wells intersect the vitric units of the Calico Hills Formation). Effective matrix porosities reported, however, are generally reliable and representative of most geologic units at YM based in part on the number of samples tested, laboratory testing methods, and size of the region sampled.

Variability in effective matrix porosity within most tuff units is usually small (table 4-1; cf., Flint, 1998). Units that showed significant variability were either thin and therefore poorly sampled, or composed of several subunits with varying porosities (Flint, 1998). In general, spatial trends in effective matrix porosities for most units were difficult to identify because of limited spatial borehole data. The two exceptions described by Flint (1998) were the middle nonlithophysal unit of the TCw, which showed a possible northwest trend of increasing porosity, and the PTn, which, although not demonstrated, is likely to show possible trending based on depositional mechanisms (pyroclastic flow or fallout deposits).

Effective fracture and fault porosities for the geologic units of the YMR were evaluated using pneumatic and gaseous tracer-tests. Porosity data reported thus far using these methods have been for locations in the BRFA and the NGDFA and are representative of conditions in close proximity to these faults. At these locations, pneumatic methods indicate that effective porosities along fault zones exceed the effective porosities of the adjacent matrix. Only small areas of these fault zones have been tested, so considerable uncertainty still exists. Application of similar methods at other locations along these faults may reduce this

uncertainty. Effective porosities for the rock matrix have also been compared to effective fracture porosities used in the site-scale UZ groundwater flow model. These comparisons show the effective fracture porosities used in the site-scale UZ groundwater flow model underestimate the minimum observed effective matrix porosities by 1–2 orders of magnitude. This discrepancy may be a combination of the limited number of pneumatic tests performed, limitations in pneumatic test interpretation methods, or uncertainty in the input model parameters of the site-scale UZ groundwater flow model.

Currently, few data exist with regard to possible changes in effective matrix and fracture porosities that may occur in the vicinity of the drifts following repository closure. During this period, it is generally assumed thermal processes associated with the waste will lead to refluxing of moisture in the vicinity of the repository, and mechanical deformation of the rock surrounding the repository will occur. Possible changes in effective matrix porosities owing to possible precipitation and dissolution processes associated with refluxing are not well understood. Mechanical deformation of rock surrounding drifts can lead to modifications of fracture apertures; the impacts of which also are not well understood.

Rock-matrix porosities for the saturated volcanic tuff formations have been characterized as well as reasonably can be expected. Additionally, so long as flow in the saturated tuffs is conservatively assumed to occur mainly in fractures, PA calculations show matrix porosity is of minor importance to repository performance calculations. Therefore, barring changes to SZ flow and transport modeling approaches, the matrix porosity data for the saturated tuff formations provided by Flint (1998) should be considered sufficient.

Estimates of effective flow porosity in the saturated tuffs are much more uncertain. This uncertainty may be reduced somewhat when data and interpretations are made available from the tracer-tests conducted in the Prow Pass interval of the C-Holes Complex. Unless an innovative interpretation approach is adopted, however, effective flow porosity estimates from these tests likely will be biased by the same factors previously discussed for the tracer-tests in the Bullfrog Tuff. The simple fact is that effective flow porosity is an extremely difficult parameter to assess in heterogenous fractured-rock formations.

Winterle and La Femina (1999) suggested that the rather high effective porosity estimates obtained from tracer-tests at the C-Holes Complex could be validated by conducting an additional test with tracer circulation in the direction of the background hydraulic gradient. The C-Holes Complex has since been decommissioned, however, so such a test does not seem likely. Thus, as discussed earlier, what remains is a range of uncertainty regarding effective porosity of the saturated tuffs that reasonably can be expected to fall within an order of magnitude range 0.001–0.01. This range of uncertainty is not likely to be reduced significantly without great expenditure of resources. The relative importance of effective flow porosity in the tuff aquifer is not clear yet because portions of the SZ flow paths through valley-fill alluvium remain to be characterized. The present level of uncertainty may be good enough, however, provided that PA analyses conducted by DOE demonstrate consideration of the effective flow porosity in the tuff aquifer at the low end of this range.

Currently, little is known about the effective porosities of the unit that make up the valley-fill located south of YM. On the basis of geological, geophysical, and well-logging data, it is known that the valley-fill is composed of spatially varying thicknesses of cobbles, gravels, sands, silts, and clays. As a result, the distributions of effective porosities are expected to show considerable spatial variability. It is hoped that in

the near future, activities associated with the Nye County Drilling Program will yield data on the spatial distribution of effective porosities in the valley-fill deposits.

5 SUMMARY AND CONCLUSIONS

This report provides in-depth discussions of porosity, its distribution in the vicinity of YM, Nevada, and its potential impact on the performance of a HLW repository located at YM. The following summarizes some of the more important aspects of this report.

Several classes of porosity are commonly identified in the porous media literature. Of these, effective primary (matrix) porosity and effective secondary (fracture and fault) porosity are important to repository performance because of their impacts on groundwater flow and radionuclide transport. Effective porosity is important because it controls groundwater flow velocities and, hence, travel times between source and compliance points. For example, given a constant groundwater flux, increases in effective porosity result in decreases in groundwater velocity and increases in travel time between source and compliance points. For radionuclides, increased travel times result in reduced radionuclide concentrations at compliance points because of radionuclide decay. Groundwater velocity controls not only the advective or bulk velocity of solutes being transported by the groundwater system but also the amount of dispersion or spreading these solutes undergo during transport. In general, the higher the velocity, the greater the dispersion. Effective porosity is also positively correlated to geochemical processes—such as the amount of mass sorbed onto the porous matrix—that attenuate radionuclide concentrations along the transport pathway. As a result, effective porosity may play an important role in repository performance.

The importance of porosity on repository performance has been investigated to varying degrees by the DOE and NRC. Using the TPA code, NRC performed a series of sensitivity analyses to look at the relative importance of model parameters on repository performance. The analyses showed that for the basecase, the effective porosity of the saturated valley-fill (alluvium) south of the repository ranked among the top twenty model parameters influencing repository performance after both 10,000 and 50,000 yrs (Mohanty et al., 1999, tables 4-1 and 4-2). In the DOE-VA, effective porosity was identified as one of the transport parameters that should be given high priority (Civilian Radioactive Waste Management System, Management and Operating Contractor, 1998, table 3-19).

To account for the potential impacts of porosity on repository performance, an understanding of the distributions of porosity in the vicinity of YM is essential. In this report, a review was performed of porosity variations in the major geologic units at YM and along the projected groundwater flow and radionuclide transport pathways away from the site. The review demonstrates that effective porosity varies across, as well as within, geologic units. In addition, the review identifies data that may be used to quantify the two general classes of porosity observed at the site. These data may be used to calibrate and validate groundwater flow and transport models for the site. In addition, these data also may be used to better constrain input parameters to PA models.

Effective porosity distributions in the near-surface are extremely important for constraining both the volume and distribution of infiltrating fluxes, which ultimately contribute to deep percolation fluxes. Methods for measuring effective matrix porosities of soils and near-surface bedrock are generally reliable, however, there are concerns that biases in soil sampling procedures may overpredict estimates of effective matrix porosities for some soil groups and, as a result, overestimate soil moisture capacity. Such overestimation may result in underprediction of infiltration fluxes. Effective fracture porosities of near-surface bedrocks also control the distribution and volume of infiltrating fluxes. Currently, estimates of effective fracture porosities of near-surface bedrock are uncertain. Because of these uncertainties, process models used to evaluate infiltration

for PA abstractions should consider a range of parameter values to ensure shallow infiltration fluxes are not underestimated.

Porosities of the tuff units of the UZ are important because they (i) influence the volume and distribution of deep percolation fluxes; (ii) influence radionuclide retardation processes, such as sorption, in units below the repository horizon; (iii) form the basis for the estimation of UZ flow parameters, such as saturated hydraulic conductivity; and (iv) provide the basis on which lithologic units in the UZ are classified. Hence, accurate estimation of porosity within the UZ tuffs is important. A large database, consisting of over 4,000 effective matrix porosity estimates, has been compiled based on well cores extracted during drilling activities in the tuffs. Although sampling procedures may not have been optimal in some units, the database nonetheless represents a significant and important source of porosity data sufficient to bound effective matrix porosities for most UZ units, with the possible exception of the vitric units of CHn, which were sampled by wells at only two locations. In general, effective matrix porosity values ranged from, on average, above 40 percent for the PTn and 30 percent the CHn, and on average less than 9 percent for the TCw and 10 percent for the TSw.

High matrix porosities in the UZ (e.g., PTn and CHn) are generally advantageous for repository performance because, during conditions of low matrix saturation, high matrix porosities may significantly reduce groundwater fluxes along fractures through imbibition processes. This reduction may significantly decrease potential radionuclide fluxes migrating from the repository horizon. In addition, in the CHn, the observed high effective matrix porosities of the permeable vitric units provide great sorption capacity for attenuation of radionuclide concentrations. It is hoped that work currently ongoing at the Busted Butte tracer-test site may provide additional information regarding effective matrix and fracture porosity data for the CHn.

Limited data are available on effective fracture and fault porosities for the geologic units of the UZ. It is known that existing estimates have been obtained using pneumatic and gaseous tracer-tests. Thus far, porosity data reported based on these methods have been for single locations in the BRFA and the NGDFA, and may represent conditions only in close proximity to these faults. At these locations, estimates of effective porosities within fault zones significantly exceed those of adjacent rock matrix. Application of similar pneumatic methods at other fault locations should reduce this uncertainty.

Currently, not many data exist from which to assess possible changes in effective matrix and fracture porosities that may occur around drifts following repository closure. It is generally assumed, however, that thermal processes associated with the waste will lead to refluxing of moisture in the vicinity of the repository and that mechanical deformation of the rock surrounding the repository will occur. Changes in effective matrix porosities that may occur in the rock surrounding the drift because of possible mineral precipitation and dissolution processes associated with refluxing are not well understood. Additionally, mechanical deformation of the rock surrounding the repository can lead to changes in fracture apertures; the effects of which also are not well understood.

In the SZ, rock-matrix porosities for the saturated volcanic tuff formations have been characterized as well as reasonably can be expected. Additionally, so long as flow in the saturated tuffs is conservatively assumed to occur mainly in fractures, PA calculations show SZ matrix porosity is of minor importance to repository performance calculations. Therefore, barring changes to SZ flow and transport modeling approaches, the matrix porosity data for the saturated tuff formations provided by Flint (1998) should be considered sufficient.

Estimates of effective flow porosity in the saturated tuffs are much more uncertain. This uncertainty may be reduced somewhat when data and interpretations are made available from the tracer-tests conducted in the Prow Pass interval of the C-Holes Complex. Unless an innovative interpretation approach is adopted, however, effective flow porosity estimates from these tests likely will be biased by the same factors previously discussed for the tracer-tests in the Bullfrog Tuff. The simple fact is that effective flow porosity is an extremely difficult parameter to assess in heterogenous fractured-rock formations.

Winterle and La Femina (1999) suggested that the rather high effective porosity estimates obtained from tracer-tests at the C-Holes Complex could be validated by conducting an additional test with tracer circulation in the direction of the background hydraulic gradient. The C-Holes Complex has since been decommissioned, however, so such a test does not seem likely. Thus, as discussed earlier, what remains is a range of uncertainty regarding effective porosity of the saturated tuffs that reasonably can be expected to fall within the range 0.001–0.01. This range of uncertainty is not likely to be reduced significantly without great expenditure of resources. The relative importance of effective flow porosity in the tuff aquifer is not clear yet because portions of the SZ flow paths through valley-fill alluvium remain to be characterized. The present level of uncertainty may be good enough, however, provided that PA analyses conducted by DOE demonstrate consideration of the effective flow porosity in the tuff aquifer at the low end of this range.

Currently, little is known about the effective porosities of the unit that make up the valley-fill south of YM. On the basis of geological, geophysical, and well-logging data, it is known that the valley-fill is composed of spatially varying thicknesses of cobbles, gravels, sands, silts, and clays. As a result, the distributions of effective porosities are expected to show considerable spatial variability. It is hoped that in the near future, activities associated with the Nye County Drilling Program will yield data on the spatial distribution of effective porosities in the valley-fill deposits.

5.1 FUTURE WORK

Future activities designed to reduce uncertainty and to lead to issue resolution regarding effective porosities at the YM site should include

- A careful review of all pneumatic data used to infer fracture porosities at the site in an effort to better constrain these estimates
- A careful review of the pneumatic and gaseous tracer testing methods to identify the reliability and limitations of each method
- A review of future well-logging data and other data that may be used to estimate effective porosities for the valley-fill units
- A review of geostatistical analyses of porosity presented in the recently released Rock Properties Report (Civilian Radioactive Waste Management System, Management and Operating Contractor, 2000).

6 REFERENCES

Ahlers, C.F., S. Finsterle, and G.S. Bodvarsson. Characterization and prediction of subsurface pneumatic response at Yucca Mountain, Nevada. *Journal of Contaminant Hydrology* 38: 47–68. 1999.

Anderson, L.A. *Rock Property Analysis of Core Samples from the Calico Hills UE25A-3 Borehole, Nevada Test Site, Nevada.* U.S. Geological Survey Open-File Report 81-1337. 1981a.

Anderson, L.A. *Rock Property Analysis of Core Samples from the Yucca Mountain UE25A-1 Borehole, Nevada Test Site, Nevada.* U.S. Geological Survey Open-File Report 81-1338. 1981b.

Anderson, L.A. *Rock Property Measurements on Large-Volume Core Samples from Yucca Mountain Usw GU-3/G-3 and USW G-4 Boreholes, Nevada Test Site, Nevada.* U.S. Geological Survey Open-File Report 84-552. 1984.

Anderson, L.A. *Results of Rock Property Measurements Made on Core Samples from Yucca Mountain Boreholes, Nevada Test Site, Nevada.* U.S. Geological Survey Open-File Report 90-474. 1991.

Anderson, L.A. *Water Permeability and Related Rock Properties Measured on Core Samples from the Yucca Mountain USW GU-3/G-3 and USW G-4 Boreholes, Nevada Test Site, Nevada.* U.S. Geological Survey Open-File Report 92-201. 1994.

Bear, J., and A. Verruijt. *Modeling Groundwater Flow and Pollution.* Dordrecht, The Netherlands: D. Reidel Publishing Company. 1987.

Bish, D.L., and S.J. Chipera. *Revised Mineralogic Summary of Yucca Mountain, Nevada.* LA–11497–MS. Los Alamos, NM: Los Alamos National Laboratory. 1989.

Bredehoeft, J.D. Fault permeability near Yucca Mountain. *Water Resources Research* 33(2): 459–2,463. 1997.

Brusseau, M.L., R.E. Jessup, and P.S.C. Rao. Modeling the transport of solutes influenced by multiprocess non-equilibrium. *Water Resources Research* 25(9): 1,971–1,988. 1989.

Civilian Radioactive Waste Management System, Management and Operating Contractor. *Total System Performance Assessment—Viability Assessment (TSPA-VA) Analyses Technical Basis Document.* B00000000–01717–4301–00007. Las Vegas, NV: TRW Environmental Safety Systems, Inc. 1998.

Civilian Radioactive Waste Management System, Management and Operating Contractor. *Simulation of Net Infiltration for Modern and Potential Future Climates.* ANL–NBS–HS–000032. Revision 00a. Las Vegas, NV: Office of Civilian Radioactive Waste Management System, Management and Operating Contractor. 1999a.

Civilian Radioactive Waste Management System, Management and Operating Contractor. *Development of Numerical Grids for UZ Flow and Transport Modeling.* ANL-NBS-HS-000015. Revision 00. Las Vegas, NV: Office of Civilian Radioactive Waste Management System, Management and Operating Contractor. 1999b.

Civilian Radioactive Waste Management System, Management and Operating Contractor. *Probability Distribution for Flowing Interval Spacing.* ANL-NBS-MD-000003. Revision 00. Las Vegas, NV: Office of Civilian Radioactive Waste Management System, Management and Operating Contractor. 1999c.

Civilian Radioactive Waste Management System, Management and Operating Contractor. *Rock Properties Model.* MDL-NBS-GS-000004. Revision 00. Las Vegas, NV: Office of Civilian Radioactive Waste Management System, Management and Operating Contractor. 2000.

Czarnecki, J.B., and R.K. Waddell. *Finite-element Simulations of Groundwater Flow in the Vicinity of Yucca Mountain, Nevada–California.* U.S. Geological Survey Water Resources Investigations Report 84-4349. 1984.

Davis, S.N. Porosity and permeability of natural materials. *Flow through Porous Media.* R.J.M. De Weist, ed. New York: Academic Press, Inc.: 54–89. 1969.

Day, W.C., C.J. Potter, D. Sweetkind, R.P. Dickerson, and C.A. San Juan. *Bedrock Geologic Map of the Central Block Area, Yucca Mountain, Nye County, Nevada.* U.S. Geological Survey Miscellaneous Investigations Series, Map I–2601. Scale 1:6000. 1998a.

Day, W. C., R.P. Dickerson, C.J. Potter, D.S. Sweetkind, C.A. San Juan, R.M. Drake, II., and C.J. Fridrich, *Geologic Map of the Yucca Mountain Area, Nye County, Nevada.* U.S. Geological Survey Geological Investigations Series, Map I–2627. Scale 1:24,000. 1998b.

de Marsily, G. *Quantitative Hydrogeology.* San Diego, CA: Academic Press, Inc. 1986.

Domenico, P.A., and F.W. Schwartz. *Physical and Chemical Hydrogeology.* New York: John Wiley & Sons. 1990.

Ervin, E.M., R.R. Luckey, and D.J. Burkhardt. Summary of revised potentiometric-surface map for Yucca Mountain and vicinity, Nevada. *Proceedings of the Fourth Annual International Conference on High-Level Radioactive Waste Management.* La Grange Park, IL: American Nuclear Society: 1,554–1,558. 1993.

Ervin, E.M., R.R. Luckey, and D.J. Burkhardt. *Revised Potentiometric-Surface Map, Yucca Mountain and Vicinity, Nevada.* U.S. Geological Survey Water Resources Investigations Report 93-4000. 1994.

Fabryka-Martin, J.T., H.J. Turin, A.V. Wolfsberg, D. Brenner, P.R. Dixon, and J.A. Musgrave. *Summary Report of Chlorine-36 Studies.* LA–CST–TIP–96–003. Yucca Mountain Project Milestone Report 3782M. Los Alamos, NM: Los Alamos National Laboratory. 1996.

Farrell, D.A., A. Armstrong, J.R Winterle, D.R. Turner, D.A. Ferrill, J.A. Stamatakos, N.C. Coleman, M.B. Gray, and S. Sandberg. *Structural Controls on Groundwater Flow in the Yucca Mountain Region*. San Antonio, TX: Center for Nuclear Waste Regulatory Analyses. 1999.

Farrell, D.A., P. La Femina, A. Armstrong, S. Sandberg, and N. Rogers. Constraining hydrogeologic models using geophysical techniques: Case study Fortymile Wash and Amargosa Desert, Southern Nevada. M.H. Powers, A. Ibrahim, and L. Cramer, eds. *Proceedings of the Symposium on the Applications of Geophysics to Engineering and Environmental Problems, 2000 Conference, Arlington, Virginia, February 20–24, 2000*. Englewood, CO: Environmental and Engineering Geophysical Society: 213–222. 2000.

Ferrill, D.A., J.A. Stamatakos, S.M. Jones, B. Rahe, H.L. McKague, R. Martin, and A.P. Morris. Quaternary slip history of the Bare Mountain Fault (Nevada) from the morphology and distribution of alluvial fan deposits. *Geology* 24: 559–562. 1996.

Ferrill, D.A., A.P. Morris, S.M. Jones, and J.A. Stamatakos. Extensional layer-parallel shear and normal faulting. *Journal of Structural Geology* 20: 355–362. 1998.

Fetter, F.W. *Applied Hydrogeology*. 3rd Edition. Englewood Cliffs, NJ: Prentice-Hall, Inc. 1994.

Fischer, J.M. *Sediment Properties and Water Movement through Shallow Unsaturated Alluvium at an Arid Site for Disposal of Low-Level Radioactive Waste Near Beatty, Nye County, Nevada*. U.S. Geological Survey Water Resources Investigations Report 92-4032. 1992.

Flint, L.E. *Characterization of Hydrogeologic Units Using Matrix Properties, Yucca Mountain, Nevada*. U.S. Geological Survey Water Resources Investigations Report 97-4243. 1998.

Flint, L.E., and A.L. Flint. *Preliminary Permeability and Water-Retention Data for Nonwelded and Bedded Tuff Samples, Yucca Mountain Area, Nye County, Nevada*. U.S. Geological Survey Open-File Report 90-569. 1990.

Flint, L.E., A.L. Flint, C.A. Rautman, and J.D. Istok. *Physical and Hydrologic Properties of Rock Outcrop Samples at Yucca Mountain, Nevada*. U.S. Geological Survey Open-File Report 95-280. 1996a.

Flint, A.L., J.A. Hevesi, and L.E. Flint. *Conceptual and Numerical Model of Infiltration for the Yucca Mountain Area, Nevada*. U.S. Geological Survey Water Resources Investigations Report. DRAFT. 1996b.

Freeze, R.A., and J.A. Cherry. *Groundwater*. Englewood Cliffs, NJ: Prentice-Hall, Inc. 1979.

Fridrich, C.J., W.W. Dudley, Jr., and J.S. Stuckless. Hydrogeologic analysis of the saturated-zone ground water system, under Yucca Mountain, Nevada. *Journal of Hydrology* 154: 133–168. 1994.

Geldon, A.L. *Preliminary Hydrogeologic Assessment of Boreholes UE-25c#1, UE25c#2, and UE25c#3, Yucca Mountain, Nye County, Nevada*. U.S. Geological Survey Water Resources Investigations Report 92-4016. 1993.

Geldon, A.L. *Results and Interpretation of Preliminary Aquifer Tests in Boreholes UE-25c#1, UE25c#2, and UE25c#3, Yucca Mountain, Nevada.* U.S. Geological Survey Water Resources Investigations Report 94-4177. 1996.

Geldon, A.L., A.M.A. Umari, M.F. Fahy, J.D. Earle, J.M. Gemmel, and J. Darnell. *Results of Hydraulic and Conservative Tracer Tests in Miocene Tuffaceous Rocks at the C-Hole Complex, 1995 to 1997, Yucca Mountain, Nevada.* Yucca Mountain Project Milestone Report SP23PM3. Las Vegas, NV: Yucca Mountain Project Office. 1997.

Geomatrix Consultants, Inc. *Saturated Zone Flow and Transport Expert Elicitation Meeting, January, 1998.* Civilian Radioactive Waste Management System, Management and Operating Contractor Report. San Francisco, CA: Geomatrix Consultants, Inc. 1998.

Hassan, A., J.H. Cushman, and J.W. Delleur. Significance of porosity variability to transport in heterogeneous porous media. *Water Resources Research* 34(9): 2,249–2,259. 1998.

Huang, K., Y.W. Tsang, and G.S. Bodvarsson. Simultaneous inversion of air-injection tests in fractured unsaturated tuff at Yucca Mountain. *Water Resources Research* 35(8): 2,375–2,386. 1999.

Illman W.A., D.L. Thompson, V.V. Vesselinov, G. Chen, and S.P. Neuman. *Single- and Cross-Hole Pneumatic Tests in Unsaturated Fractured Tuffs at the Apache Leap Research Site: Phenomenology, Spatial Variability, Connectivity, and Scale.* NUREG/CR–5559. Washington, DC: Nuclear Regulatory Commission. 1998.

Klavetter, E.A., and R.R. Peters. *An Evaluation of the Use of Mercury Porosimetry in Calculating Hydrologic Properties of Tuffs from Yucca Mountain, Nevada.* SAND86–0286. Albuquerque, NM: Sandia National Laboratories. 1987.

Kume, J., and D.P. Hammermeister. *Geohydrologic Data from Test Hole USW UZ-7, Yucca Mountain Area, Nye County, Nevada.* U.S. Geological Survey Open-File Report 88-465. 1990.

LeCain, G.D. *Results from Air-Injection and Tracer Testing in the Upper Tiva Canyon, Bow Ridge Fault, and Upper Paintbrush Contact Alcoves of the Exploratory Studies Facility, August 1994 through July 1996, Yucca Mountain, Nevada.* U.S. Geological Survey Water Resources Investigations Report 98-4058. 1998.

LeCain, G.D., L.O. Anna, and M.F. Fahy. *Results from Geothermal Logging, Air and Core-Water Chemistry Sampling, Air-Injection Testing and Tracer Testing in the northern Ghost Dance Fault, Yucca Mountain, Nevada, November 1996 to August 1998.* U.S. Geological Survey Water Resources Investigations Report 99-4210. 1999.

Loskot, C.L. *Geohydrologic Data from Test Hole USW UZ-6S, Yucca Mountain, Nye County, Nevada.* U.S. Geological Survey Open-File Report 93-60. 1993.

Loskot, C.L,. and D.P. Hammermeister. *Geohydrologic Data from Test Holes UE-25, UZ#4, and UZ#5, Yucca Mountain Area, Nye County, Nevada.* U.S. Geological Survey Open-File Report 90-369. 1992.

Luckey, R.R., P. Tucci, C.C. Faunt, E.M. Ervin, W.C. Steinkampf, F.A. D'Agnese, and G.L. Patterson. *Status of Understanding of the Saturated-Zone Ground-Water Flow System at Yucca Mountain, Nevada, As of 1995*. U.S. Geological Survey Water Resources Investigations Report 96-4077. 1996.

Moench, A.F. Convergent radial dispersion in a double-porosity aquifer with fracture skin: Analytical solution and application to a field experiment in fractured chalk. *Water Resources Research* 31(8): 1,823–1,835. 1995.

Mohanty, S., and T.J. McCartin. *Total-system Performance Assessment (TPA) Version 3.2 Code: Module Descriptions and User's Guide*. San Antonio, TX: Center for Nuclear Waste Regulatory Analyses. 1998.

Mohanty, S., R. Codell, R.W. Rice, J. Weldy, Y. Lu, R.M. Byrne, T.J. McCartin, M.S. Jarzemba, and G.W. Wittmeyer. *System-Level Repository Sensitivity Analyses Using TPA Version 3.2*. CNWRA 99-002. San Antonio, TX: Center for Nuclear Waste Regulatory Analyses. 1999.

Nelson, P.H. *Computation of Porosity and Water Content from Geophysical Logs, Yucca Mountain, Nevada*. U.S. Geological Survey Open-file Report 96-078. 1996.

Nelson, P.H., D.C. Muller, U. Schimschal, and J.E. Kilber. *Geophysical Logs and Core Measurements from Forty Boreholes at Yucca Mountain, Nevada*. U.S. Geological Survey Geophysical Investigations Series, Map GP–1001. 1991.

Nuclear Regulatory Commission. *Issue Resolution Status Report (Key Technical Issue: Unsaturated and Saturated Flow Under Isothermal Conditions)*. Revision 1. Washington, DC: Nuclear Regulatory Commission. 1998.

Nuclear Regulatory Commission. *Issue Resolution Status Report (Key Technical Issue: Unsaturated and Saturated Flow Under Isothermal Conditions)*. Revision 2. Washington, DC: Nuclear Regulatory Commission. 1999.

Oatfield, W.J., and J.B. Czarnecki. Hydrogeologic inferences from driller's logs and from gravity and resistivity surveys in the Amargosa Desert, Southern Nevada. *Journal of Hydrology* 124: 131–158. 1991.

Patterson, G.L., E.P. Weeks, J.P. Rousseau, and T.A. Oliver. *Interpretation of Pneumatic and Chemical Data from the Unsaturated Zone near Yucca Mountain, Nevada*. U.S. Geological Survey D–AI08–92–NV10874. 1996.

Peters, R.R., E.A. Klavetter, I.J. Hall, S.C. Blair, P.R. Heller, and G.W. Gee. *Fracture and Matrix Hydraulic Characteristics of Tuffaceous Materials from Yucca Mountain, Nye County, Nevada*. SAND84–1471. Albuquerque, NM: Sandia National Laboratories. 1984.

Peyton, G.H., J.P. Gibb, M.H. Lafaivre, and J.D. Ritchey. On the concept of effective porosity and its measurement in saturated fine-grained materials. *Proceedings of the Second Annual Canadian/American Conference on Hydrogeology: Hazardous Wastes in Groundwater—A Soluble Dilemma, June 25-29, 1985*. Banff, Alberta, Canada: Alberta Research Council. 1985.

Plume, R.W. *Hydrogeologic Framework for the Great Basin Region of Nevada, Utah, and Adjacent States.* U.S. Geological Survey Professional Paper 1409-B. 1996.

Rautman, C.A., and S.A. McKenna. *Three-Dimensional Hydrological and Thermal Property Models of Yucca Mountain, Nevada.* SAND97–1730. Albuquerque, NM: Sandia National Laboratories. 1997.

Rautman, C.A., L.E. Flint, A.L. Flint, and J.D. Istok. *Physical and Hydrologic Properties of Outcrop Samples from a Nonwelded to Welded Tuff Transition, Yucca Mountain, Nevada.* U.S. Geological Survey Open-File Report 95-4061. 1995.

Reimus, P.W., M.J. Haga, T. Callahan, I. Anghel, H.J. Turin, and D. Counce. *C-Holes Update Report: Reinterpretation of the Reactive Tracer Test in the Bullfrog Tuff and Results of Laboratory Testing.* DRAFT. Yucca Mountain Project Milestone Report SP32E2M4. Los Alamos, NM: Los Alamos National Laboratory. 1998.

Robison, J.H. Structure of pre-Cenozoic rocks in the vicinity of Yucca Mountain, Nye County, Nevada—A Potential Nuclear-Waste Disposal Site. *U.S. Geological Survey Bulletin 1647.* 1984.

Rousseau, J.P., C.L. Loskot, F. Thamir, and N. Lu. *Results of Borehole Monitoring in the Unsaturated Zone within the Main Drift Area of the Exploratory Studies Facility, Yucca Mountain, Nevada.* Yucca Mountain Project Level 3 Milestone Report SPH22M3. Las Vegas, NV: Yucca Mountain Project Office. 1997a.

Rousseau, J.P., E.M. Kwicklis, and D.C. Gillies. *Hydrogeology of the Unsaturated Zone, North Ramp Area of the Exploratory Studies Facility, Yucca Mountain, Nevada.* U.S. Geological Survey Water Resources Investigations Report 98-4050. 1997b.

Rush, F.E., W. Thordarson, and L. Bruckheimer. *Geohydrologic and Drill-Hole Data for Test Well USW H-1, Adjacent to the Nevada Test Site, Nye County, Nevada.* U.S. Geological Survey Open-File Report 83-141. 1983.

Sawyer, D.R., R.J. Fleck, M.A. Lanphere, R.G. Warren, D.E. Broxton, and M.R. Hudson. Episodic caldera volcanism in the Miocene southwestern Nevada volcanic field: Revised stratigraphic framework, 40Ar/39Ar geochronology, and implications for magnetism and extension. *Geological Society of America Bulletin 106*: 1,304–1,318. 1994.

Sonnenthal, E.L., C. Ahlers, and G. Bodvarsson. Fracture and fault properties for the unsaturated zone site-scale flow model. *The Site-Scale Unsaturated Zone Model of Yucca Mountain, Nevada, for the Viability Assessment.* G. Bodvarsson, T. Bandurraga, and Y. Wu, eds. LBNL–40376. Berkeley, CA: Lawrence Berkeley National Laboratory. 1997.

Stamatakos, J.A., C.B. Connor, and R.H. Martin. Quaternary basin evolution and basaltic magnetism of Crater Flat, Nevada, from detailed ground magnetic surveys of the Little Cones. *Journal of Geology* 105: 319–330. 1997.

Stothoff, S. *Infiltration Abstractions for Shallow Soil over Fractured Bedrock in a Semiarid Climate.* San Antonio, TX: Center for Nuclear Waste Regulatory Analyses. 1999.

Tsang, Y.W., J. Wang, B. Freifeld, P. Cook, R. Suarez-Rivera, and T. Tokunaga. *Letter Report on Hydrological Characterization of the Single Heater Test Area in the Exploratory Studies Facility, Yucca Mountain Site Characterization Project Report.* Berkeley, CA: Lawrence Berkeley National Laboratory. 1996.

Vesselinov, V.V. and S.P. Neuman. Numerical inverse interpretation of multistep transient single-hole pneumatic tests in unsaturated fractured tuffs at the Apache Leap Research Site. *Theory, Modeling and Field Investigations in Hydrogeology: a Special Volume in Honor of Shlomo P. Neuman's 60th Birthday.* Boulder, CO: Geological Society of America. 2000.

Walker, G.E., and T.E. Eakin. *Geology and Ground Water of Amargosa Desert, Nevada–California.* Ground-Water Resources-Reconnaissance Series, Report 14, Geological Survey. Las Vegas, NV: U.S. Department of the Interior. 1963.

Wang, J.S.Y., P.J. Cook, R.C. Trautz, R. Salve, A.L. James, S. Finsterle, T.K. Tokunaga, R. Solbau, J. Clyde, A.L. Flint, and L.E. Flint. *Field Testing and Observation of Flow Paths in Niches: Status Report of the Drift Seepage Test and Niche Moisture Study.* Yucca Mountain Project Level 4 Milestone Report SPC314M4. Las Vegas, NV: Yucca Mountain Project Office. 1997.

Weeks, E.P., and W.E. Wilson. *Preliminary Evaluation of Hydrologic Properties of Cores of Unsaturated Tuff, Test Well USW H-1, Yucca Mountain, Nevada.* U.S. Geological Survey Water Resources Investigations Report 84-4193. 1984.

Whitfield, M.S., Jr., W. Thordarson, and E.P. Eshom. *Geohydrologic and Drill-Hole Data for Test Well USW H-4, Yucca Mountain, Nye County, Nevada.* U.S. Geological Survey Open-File Report 84-449. 1984.

Winograd, I.J., and W. Thordarson. *Hydrogeologic and Hydrochemical Framework, South-Central Great Basin, Nevada–California, with Special Reference to the Nevada Test Site.* U.S. Geological Survey Professional Paper 712-2. 1975.

Winterle, J.R., and P.C. La Femina. *Review and Analyses of Hydraulic and Tracer Testing at the C-Holes Complex Near Yucca Mountain, Nevada.* San Antonio, TX: Center for Nuclear Waste Regulatory Analyses. 1999.

Winterle, J.R., and W.M. Murphy. Time scales for dissolution of calcite fracture fillings and implications for saturated zone radionuclide transport at Yucca Mountain, Nevada. *Proceedings of the Scientific Basis for Nuclear Waste Management XXII Symposium–Fall 1998 Meeting.* Warrendale, PA: Materials Research Society: 713–720. 1999.

Winterle, J.R., R.W. Fedors, D.L. Hughson, and S. Stothoff. *Review of the Unsaturated Zone Models Used to Support the Viability Assessment of a Repository at Yucca Mountain.* San Antonio, TX: Center for Nuclear Waste Regulatory Analyses. 1999a.

Winterle, J.R., R.W. Fedors, D.L. Hughson, and S. Stothoff. *Update of Hydrologic Parameters for the Total-system Performance Assessment Code*. San Antonio, TX: Center for Nuclear Waste Regulatory Analyses. 1999b.

Winterle, J.R., N.M. Coleman, W.A. Illman, and D. Hughson. *Review of Permeability Estimates Obtained from the Yucca Mountain Project*. San Antonio, TX: Center for Nuclear Waste Regulatory Analyses. 2000.

Witherspoon, P.A., J.S.Y. Wang, K. Iwai, and J.E. Gale. Validity of the Cubic Law for fluid flow in a deformable rock fracture. *Water Resources Research* 16: 1,016–1,024. 1980.

Yang, I.C., G.W. Rattray, P. Yu. *Interpretations of Chemical and Isotopic Data from Boreholes in the Unsaturated Zone at Yucca Mountain, Nevada.* U.S. Geological Survey Water Resources Investigations Report 96-4058. 1996.

APPENDIX

SUMMARY OF METHODS FOR ESTIMATING POROSITY

The discussions in this appendix are focused on summarizing methods for estimating both total and effective porosities and their relative advantages and disadvantages. The methods considered will include empirical methods, core- or laboratory-scale methods and field-scale methods. Although effective porosity is the important parameter for hydrogeologic studies, total porosity is included for completeness.

1 EMPIRICAL METHODS

Attempts have been made to quantify porosity using empirical relationships. Often such relationships attempt to relate porosity to grain shape, grain composition, uniformity, and degree of compaction (Vukovic and Sorro, 1992). Vukovic and Sorro (1992) indicated that several investigations have demonstrated that grain shape has a significant impact on porosity. In general, grains of irregular shapes create vault-like structures that leave larger voids than spherical grains. In the case of grains with sharp edges, tests indicate porosity to be approximately 2–5 percent higher than for the case of spherical grains Vukovic and Soro, 1992). Of the factors that influence porosity, grain uniformity is believed to have the greatest effect. Porosity and the coefficient of uniformity data collected by various authors appear to indicate that the porosity of most soils is inversely related to the coefficient of uniformity (Vukovic and Soro, 1992, page 30, figure 5, and eq. 53). It should be noted, however, that equations described in Vukovoc and Soro (1992, eq. 53) at best provide crude estimates of porosity.

2 CORE-SCALE METHODS

Core- or laboratory-scale methods may be used to evaluate both total and effective porosities. The methods generally involve recovering cores and transferring them back to the laboratory for analysis. Although recovery and transport procedures attempt to minimize core disturbance, some disturbance nontheless occurs, which may influence estimates of porosity. In the following discussion, the focus is on methods for estimating total porosity and then on methods for estimating effective porosity.

2.1 TOTAL POROSITY

Several approaches are available for accurately estimating the porosity of soil and rock cores. The most common of these methods involve (i) measuring both the bulk density of the core, ρ_b, and the grain density of the matrix, ρ_p, and estimating the total porosity, φ_t, using simple expressions such as $\varphi_t = (1-\rho_b/\rho_p)$; and (ii) using gas pycnometers (or pyknometers).

In method (i), the particle density refers to the ratio of the total mass of the solid particles to their volume, excluding pore spaces between particles. The two most accurate method for determining particle density involves the use of a pycnometer. Blake and Hartge (1986a) (cf., American Society for Testing and Materials, 1958) provide a thorough description of this method. Although the method is accurate, the process is considered quite laborious. An alternate, cheaper approach for determining soil particle density is submersion. An in-depth discussion of this approach is provided by Blake and Hartge (1986a). The submersion method sacrifices some precision when compared to the pycnometer approach, but offers ease of measurement, especially when measurements are to be made on a series of samples. In addition, the submersion method does not require a calibrated pycnometer, and reproduceability is easily achieved. The

bulk density of soil samples readily can be determined using core methods, excavation methods, and radiation methods. Comprehensive summaries of these methods are contained in Blake and Hartge (1986b) and are not reproduced here. Of these methods, radiation methods appear to be the most robust, allowing for *in situ* measurements over short time periods with little soil disturbance; however, the method requires some degree of expertise. Although not as robust, the other methods also provide high quality bulk density estimates, but at considerably more effort.

Method (ii) provides a more rigorous but complicated approach. In this method, total porosity is determined using either a variable volume helium gas pycnometer or a constant volume helium gas pycnometer. Summaries of these methods for measuring total porosity are in Danielson and Sutherland (1986) (cf., Russell, 1950; Page, 1948). Commercially available gas pycnometers are generally capable of higher precision than that usually warranted for soil porosity measurements.

2.2 EFFECTIVE POROSITY

Several laboratory approaches exist for measuring laboratory porosity: simple volumetric measurements, mercury intrusion porosimetry, desorption methods, and laboratory diffusion experiments performed on soil and rock cores. These methods, summarized in the following paragraphs, include weight ratio methods, mercury intrusion porosimetry methods, water desorption methods, and laboratory diffusion methods.

2.2.1 Weight Ratio Methods

The weight ratio method is commonly used to estimate effective porosity because of its simplicity. This approach involves oven drying a sample of known volume of soil, V, at approximately 105 °C until it reaches a constant weight to expel moisture clinging to its surface, but not water hydrated as part of its mineral composition. The dried sample is then submerged into a known volume of water contained in a sealed chamber until fully saturated. The volume of the void space of the sample, V_v, is then assumed equal to the original water volume less the volume in the chamber after the saturated sample is removed. This laboratory procedure yields a value for the effective porosity for water because it excludes pores not large enough to contain water molecules and those not interconnected. A drawback to this approach is that it can take an exceedingly long time for low-permeability rocks to saturate in water.

2.2.2 Mercury Intrusion Porosimetry Methods

Mercury intrusion porosimetry provides another laboratory approach for estimating effective porosity as well as the distribution of pore volumes within a sample. This method characterizes the pore structure of a sample (initially evacuated to remove fluid) immersed in a pressure adjustable, mercury filled chamber. Because mercury is a nonwetting fluid for most rocks and minerals, it will not penetrate the sample's pores unless a pressure is applied. By applying known pressure increments and recording the associated volumetric changes of mercury in the container, the amount of mercury invading the pore spaces of the sample can be determined. It is assumed that each pressure increment forces mercury into the accessible pores with a range of diameters. In this manner, the volume of pore space between pressure increments, and thus diameter increments, is recorded, generating a pore-size distribution. Assuming that all pores have been intruded by mercury, the effective porosity for the sample may be calculated from the total volume of mercury that can be forced if the bulk volume of the sample is known. The advantages of mercury intrusion porosimetry

compared to most other methods are generally believed to be speed, accuracy, the ability of the method to perform analysis on a wide variety of materials, and the range of pore diameters that can be sampled (down to 0.003 μm). As discussed by Dullien (1991), the distribution of pore volumes determined from this approach may be in error owing to assumptions inherent in models commonly used to calculate pore size volumes from the data collected. Dullien (1991) demonstrated that significant differences in the distribution of pore size volumes occur when data from this method are compared to similar data collected using more accurate optical methods.

2.2.3 Water Desorption Methods

Water desorption is another approach that can be used to determine the effective porosity of a soil or rock sample. Using this method, the sample is first saturated and then drained in a series of predefined steps. At each step, the volume of water drained from the sample is measured. Using appropriate assumptions, the water removed can be equated to the soil pore volume drained and the pore size distribution determined. In theory, the largest pore volumes should drain first followed by progressively smaller pores. The theory, apparatus, and procedures that describe this method are well documented in Danielson and Sutherland (1986) who also point out several errors inherent in the method. The most significant of these errors relate to the determination of a meaningful sample volume with changing saturation and the assurance of sample saturation. Both errors can result in errors in the computed sample porosity and associated pore-size distributions.

2.2.4 Laboratory Diffusion Methods

Laboratory diffusion methods have also been used to obtain estimates of effective porosity. van der Kamp et al. (1996) presented an approach for estimating isotopic composition and chemistry of groundwater in low permeability materials that also allows the effective porosity of the material to be determined. In the analysis, the sample is placed in a radial diffusion cell and chemical exchanges between the porous medium and a reservoir located along the central axis of the sample (to which mass is added) monitored [see van der Kamp et al. (1996) for further details]. By recording chemical concentrations in the reservoir and the mass added to the reservoir, the effective porosity of the sample may be determined using appropriate equations and assumptions [see van der Kamp et al. (1996) for further details]. An advantage of this method is that it is easy to implement and well suited to low permeability materials. However, the method has not been rigorously tested. Novakowski and van der Kamp (1996) also developed a radial diffusion cell method that allowed effective porosity to be determined. Semianalytical equations developed for the method allowed the effective porosity and the effective diffusion coefficient to be determined from measured diffusion cell data via a parameter fitting procedure. Effective porosities estimated from this method were reported by Novakowski and van der Kamp (1996), consistent with estimates obtained using other methods.

3 FIELD-SCALE METHODS

In this field-scale section, methods of estimating total porosity are first discussed followed by field-scale methods for estimating effective porosity.

3.1 TOTAL POROSITY

Several geophysical logging techniques provide estimates of total porosity. The following sections present discussions of some of the more commonly used geophysical logging methods. More in-depth discussions of the individual techniques are available in Keys (1989) and Daniels and Keys (1990). Finally, to constrain porosity estimates, it is generally advisable to use several different logging methods.

3.1.1 Geophysical Logging Methods

Total porosity affects the response of a number of geophysical methods. As a result, a common approach for investigating total porosity is geophysical logging. Although such geophysical logging methods do not measure porosity directly, they are commonly used to estimate porosity. These methods include neutron logs, gamma-gamma logs, and acoustic-velocity logs. A comprehensive summary of the impact of porosity on common logging methods is given by Keys (1989).

Gamma-gamma,and neutron logs generally allow estimates of total porosity to be determined during saturated conditions when the gamma-gamma and neutron logs are properly calibrated and standardized. Acoustic-velocity logs in most cases provide estimates of total porosity, however, in some cases, secondary porosity openings may not be detected (Keys, 1989). In crystalline rock environments, acoustic-velocity logs are routinely used to investigate the distribution and character of fractures (Keys, 1989). Because these logging methods are commonly used and described in literature, the interested reader is referred to Keys (1989), Telford et al. (1976), and Sharma (1997) for in-depth descriptions of these methods and the mechanics of estimating total porosity from the various field logs.

Apart from the traditional methods, several alternate methods exist that allow porosity estimating. One of these methods is the gravity method. By measuring gravity at stations in a borehole, estimates of the mean bulk formation density can be determined. Combining this estimate with knowledge of the grain density of the matrix allows the total porosity to be estimated. The two advantages of this method for estimating total porosity are (i) the method allows a greater depth of formation penetration than traditional approaches and is, therefore, not influenced by near well damage caused by drilling and (ii) the well casing has negligible impact on the method. A major disadvantage of the method is that readings are sensitive to motion of the instrument, and in most cases this necessitates time intervals of more than ten minutes between readings.

A newer nonstandard tool for logging formation porosity is the Accelerator Porosity Sonde, which uses a powerful electronic source instead of the chemical sources common in the more traditional neutron logging tools.[1] Total porosity values estimated by this method are less sensitive to lithologic effects common in more traditional neutron logging probes. Because of the an additional eccentralizing bow-spring design, the tool is less influenced by borehole irregularities. The tool provides two porosity measurements, one corrected for borehole conditions and tool standoff that is nearly independent of lithologic effects and another that is similar to that obtained from more traditional neutron logging tools.

[1] See http://www.ldeo.columbia.edu/BRG/ODP/LOGGING/TOOLS/aps.html.

In general, for meaningful porosity estimates to be obtained from geophysical logs, a number of procedures and corrections must be adhered to. Foremost among these are proper calibration and standardization of logs and proper well construction and development practices.

3.1.1.1 Calibration and Standardization of Geophysical Logs

If geophysical logs are to be used for any type of quantitative analysis, such as porosity estimation, they need to be properly calibrated and standardized to help establish comparability between logs made with differing equipment (Keys, 1989). Calibration is the process of establishing environmental values for log responses in a semi-infinite model that simulates the natural environment in the vicinity of the well (Keys, 1989). In this context, environmental values are related to physical properties of the porous medium such as porosity or acoustic velocity. Hence, probe response calibration needs to be accomplished in a medium that closely simulates the chemical and physical compositions of the materials to be measured. Calibration is commonly performed before and after logging. Standardization is the process of checking the response of the logging probes at the well site before and after logging. Comprehensive discussions of standardization and calibration for the various geophysical logging techniques are beyond the scope of this report and the interested reader is referred to Keys (1989).

3.1.1.2 Well Construction and Development

Well construction and development practices are important to the accurate estimation of porosity. One aspect of well construction that plays an important role in the reliable determination of total porosity is borehole diameter. Although many logs are titled borehole-compensated or borehole-corrected, almost all logs are affected to varying degrees by substantial changes in borehole diameter (Keys, 1989). Such substantial changes in well diameter, if not accounted for, can result in significant errors in porosity estimates. For this reason, high quality borehole caliper logs need to be run in conjunction with geophysical logging.

Well cementing and gravel packing also affect total porosity estimates when well logs are performed after well completion. For example, material in gravel packs may become heterogeneous because of slumping of material from the rockwall, or nonuniformity in the cement and the gravel pack may occur. If undetected, these can significantly impact the porosities determined from the well logs.

3.2 EFFECTIVE POROSITY

Several approaches may be used to obtain field-scale estimates of effective porosity: well logging methods, tracer-test methods, pump-test methods, and pneumatic methods.

3.2.1 Geophysical Logging Methods

Electrical resistivity logs, when properly calibrated and standardized, may provide estimates of effective porosity when no highly electrically conductive mineral grains are present in the matrix. Of the electrical resistivity logging techniques available, "normal-resistivity" or "conventional-resistivity" logging, which consists of a four-electrode spread (two current and two voltage electrodes spaced either 16 in. or 64 in. apart), is the most commonly used in hydrogeologic investigations because of its depth of penetration and reliability. From the resistivity response and a knowledge of pore-water electrical conductivity, effective porosity is generally calculated using Archie's Law. As with the previous logging methods, estimates of

effective porosity are only meaningful during conditions of complete saturation. Because the flow of electrical current through pore spaces is affected by pore geometries, the electrical conductivity of pore fluids, and the presence of charged clay particles, resistivity may be in error in some cases when used to estimate effective porosity (Keys, 1989).

3.2.2 Tracer-Test Methods

Field-scale tracer-tests have been used to obtain field-scale transport parameters including effective porosity. Two types of field tracer-tests are common: forced-gradient tests and natural-gradient tests. In forced-gradient tests, artificial hydraulic gradients are created in the saturated zone using either injection or withdrawal wells or both. Next, tracer is injected at some fluid injection point in either an instantaneous or continuous mode and the resulting solute concentration breakthrough curve is recorded at the withdrawal well. The solute breakthrough curves are then analyzed to yield hydrologic parameters including effective matrix porosity, and where applicable, effective fracture porosity. Examples of forced-gradient tests and associated interpretations to yield transport parameter estimates including effective porosity include Reimus and Turin (1997), Garnier et al. (1985) (cf., Maloszewski and Zuber, 1990; Moench, 1995), Novakowski (1992) (cf., Novakowski and Lapcevic, 1994), Abelin et al. (1991), Gonzalez and Bentley (1984), and Birgersson et al. (1993). The advantages of the forced-gradient approach are that it is fast (on the order of days to months), and relatively cheap to perform. A potential disadvantage is that because the ambient system is disrupted, the porosity estimate may reflect the dynamic porosity of the system and not the effective porosity.

In large-scale natural-gradient tracer-tests, the chemical tracer is either emplaced or injected into the ambient groundwater flow system, and the evolving tracer plume is monitored temporally at a number of monitoring points distributed spatially along the expected tracer migration path. Several detailed natural-gradient tracer-tests involving both conservative and nonconservative tracers have been performed to date. Of these, the most widely analyzed include the Stanford-Waterloo Tracer-Test (MacKay et al., 1986), the Cape Cod Tracer-Test (LeBlanc et al., 1991), and the Columbus Air Force Base Tracer-Test (Boggs et al., 1992). One approach for estimating effective porosity from such large-scale tracer-tests is documented by Garabedian et al. (1991) for the Cape Cod Tracer-Test. These researchers estimated the field-scale effective porosity for the bromide tracer by fitting the average calculated mass from the sampled data to the known injected mass. The effective porosity estimated in this manner appears consistent with earlier estimates determined from a prior tracer-test at the site (Garabedian et al., 1988). The effective porosity estimate reported by Garabedian et al. (1988) is observed to be higher than that reported by Wolf (1988), based on core collected at the site. Hess et al. (1992) attributed this difference to core compaction during coring. Although not documented, effective porosities may also be inferred from large-scale, natural-gradient tracer-tests from estimated retardation factors.

3.2.3 Barometric Methods

Fluctuations in surface barometric pressures owing to diurnal temperature changes and meteorologic and tidal factors induce the movement of air in the unsaturated zone. The diffusive properties of soils and rocks cause the phase lag and amplitude attenuation of the barometric signal. Although the mathematical description of the phenomena was first proposed by Buckingham (1904), Stallman (1967) and Stallman and Weeks (1969) were the first to relate barometric pressure fluctuations monitored in the subsurface to the

diffusivity of geologic media; here, diffusivity is defined as the ratio of a rock's permeability to its compressible storage capacity.

Geologic media with high diffusivity (e.g., gravel, coarse sand, and highly fractured media) tend to have a minimal effect in attenuating and causing time lag in the barometric signal measured at depths, while significant attenuation and time lag are observed in subsurface materials with small diffusivities. The diffusivity of the geologic medium to air is affected by variations in water content of soils and rocks. In well drained soils, the effect of water content on the passage of barometric signals is less compared to fine grained materials with higher water contents. Thus, the value of permeability, porosity, and diffusivity obtained from well drained soils represents more closely the intrinsic properties of the medium. It should be noted that the Klinkenberg effect (1941), or gas slippage, can bias diffusivity estimates for fine grained materials with intrinsic permeabilities of 10 millidarcies or less (Weeks, 1978).

Measurements of pneumatic pressures have been made at various depths in isolated piezometers constructed in the unsaturated zone at various sites including playa sediments and basalt flows (Weeks, 1978), shallow soils (Rojstaczer and Tunks, 1995), and fractured tuffs (Rousseau et al., 1997). The time series of barometric pressure fluctuations have been analyzed using numerical methods (Weeks, 1978; Rousseau et al., 1997; Ahlers et al., 1999) and analytical techniques (e.g., Shan, 1995; Shan et al., 1999) to yield the diffusivity of the medium. Vertical permeability is estimated from the calculated diffusivity by assuming a value of porosity usually determined from laboratory analyses of cores. Although the focus has been on estimating permeability from barometric pressure fluctuations, air-filled porosity of the medium can be estimated by assuming a value of air permeability, perhaps determined from air injection tests or laboratory core analysis. Porosities and permeabilities obtained in this manner are representative of bulk, air-filled properties of the medium.

3.2.4 Transient Pneumatic Tests

Pumping or injection tests in the unsaturated zone using air are often used to determine flow properties of unsaturated soil and fractured rocks. In principle, pneumatic tests are similar to their hydraulic counterparts conducted in fully water-saturated media. Air is either injected or withdrawn from packed-off intervals, which causes a corresponding pressure increase or decrease in observation wells and packed-off intervals. The pressure response in observation wells can be related to pneumatic flow parameters such as air permeability and air-filled porosity through type-curve analysis or numerical inverse modeling.

Determination of air-filled porosity requires the transient interpretation of air injection tests. The interpretation of pneumatic tests can be more complicated particularly for single-hole tests that are more prone to nonlinear effects seen near the well. The nonlinear effects seen near the injection well are less apparent in data from cross-hole pneumatic injection tests. Commonly observed nonlinear effects include two-phase flow that arises from the capillary interaction of injected air with water and non-Darcian behavior. Air that is highly compressible also causes nonlinearities in the equations to be solved for data analysis. For purposes of data interpretation by means of analytical formulae, air compressibility is usually assumed to be constant.

A complete description of air-water interaction requires two systems of coupled partial differential equations—one for each phase. The development of corresponding analytical formulae to be used for

type-curve interpretation requires that two-phase flow be approximated by single-phase airflow and that water be treated as immobile.

Because its relatively low importance, enhanced permeability due to slip flow [the Klinkenberg (1941) effect] is usually neglected in the interpretation of well tests. The interpretation pneumatic test data based on groundwater equations is possible when slip flow can be neglected (Massmann, 1989). Estimates of air-filled porosity obtained by type-curve or numerical inverse interpretation represent the bulk air-filled porosity of the soil or rock. Reports of air-filled porosities obtained from the interpretation of pneumatic tests may be found in the literature[2,3] (Massmann and Madden, 1994; Illman et al., 1998; LeCain 1998; LeCain et al., 1999; Vesselinov and Neuman, 2000).

3.2.5 Hydraulic Pump-Test Methods

Hydraulic pump-tests in unconfined aquifers commonly display two characteristic temporal responses: (i) an early-time response in which the system behaves as a confined aquifer and water is released from elastic storage and (ii) a late-time response during which drainage of the pore spaces takes place. Application of common pump-test analytical solutions to the late-time response generally allows the specific yield of the aquifer to be determined (Neuman, 1974, 1975, 1979; Streltsova, 1974). As stated earlier, specific yield can be equated to effective porosity, particularly for coarse grained hydrostratigraphic units. Moench (1984) described a pump-test interpretation method for dual porosity systems in which fracture skin is present. Among the aquifer hydraulic parameters produced by the method are the specific storages of the matrix block and the fracture skin. From these parameters, bounding estimates for the effective porosity of the matrix and the fracture skin may be possible if the fluid density and the matrix and fracture skin compressibilities are known.

Pump-tests in unconfined aquifers may vary considerably in design and scale, with the volume of porous media sampled ranging from several tens of square meters (single well tests) to several square kilometers (multiple wells tests). Because pump-tests sample large volumes of porous media, in which varying scales of heterogeneity may exist, effective porosity values estimated from such tests are averaged values representative of the scale of measurement. That is, such values are commonly not representative of a particular geologic unit except for small-scale localized tests.

Because water released from storage in confined systems is a function of both effective porosity and formation compressibility (i.e., the early-time response of unconfined systems; see Neuman, 1974, 1975), pump-tests in such systems yield no information regarding the porosity of the system unless formation compressibility is known.

---

[2] Illman, W.A., and S.P. Neuman. Type-curve interpretation of a cross-hole pneumatic test in unsaturated fractured tuff. *Water Resources Research*. Submitted for publication. 2000.

[3] Chen, G., W.A. Illman, D.L. Thompson, V.V. Vesselinov, and S.P. Neuman. Geostatistical, Type-Curve, and Inverse Analyses of Pneumatic Injection Tests in Unsaturated Fractured Tuffs at the Apache Leap Research Site Near Superior, Arizona. *Dynamics of Fluids in Fractured Rocks—Concepts and Recent Advances, in Honor of Paul A. Witherspoon's 80th Birthday*. In press. 2000.

4 REFERENCES

Abelin, H., L. Birgersson, L. Moreno, H. Widén, T. Ågren, and I. Neretneiks. A large-scale flow and tracer experiment in granite. 2: Results and interpretation. *Water Resources Research* 27(12): 3,119–3,135. 1991.

Ahlers, C.F., S. Finsterle, and G.S. Bodvarsson. Characterization and prediction of subsurface pneumatic response at Yucca Mountain, Nevada. *Journal of Contaminant Hydrology* 38: 47–68. 1999.

American Society for Testing and Materials. *Procedures for Testing Soils*. Philadelphia, PA: American Society for Testing and Materials. 1958.

Birgersson, L., L. Moreno, I. Neretnieks, H. Widén, and T. Ågren. A tracer migration experiment in a small fracture zone in granite. *Water Resources Research* 29(12): 3,867–3,878. 1993.

Blake, G.R., and K.H. Hartge. Particle Density. *Methods of Soil Analysis. Part 1: Physical and Mineralogical Methods.* 2nd Edition. Number 9 (Part 1) in series Agronomy. A. Klute, ed. Madison, WI: Soil Science Society of America, Inc. 1986a.

Blake, G.R., and K.H. Hartge. Bulk Density. *Methods of Soil Analysis. Part 1: Physical and Mineralogical Methods.* 2nd Edition. Number 9 (Part 1) in series Agronomy. A. Klute, ed. Madison, WI: Soil Science Society of America, Inc. 1986b.

Boggs, J.M., S.C. Yound, L.M. Beard, L.W. Gelhar, K.R. Rehfeldt, and E.E. Adams. Field study of dispersion in a heterogeneous aquifer. 1: Overview and site description. *Water Resources Research* 28(12): 3,281–3,291. 1992.

Buckingham, E. Contributions to our knowledge of the aeration of soil. *U.S. Department of Agriculture Soils Bureau Bulletin* 25: 52. 1904.

Daniels, J.I., and W.S. Keys. Geophysical well logging for evaluating hazardous waste sites. *Geotechnical and Environmental Geophysics. Investigations in Geophysics, No. 5.* S.H Ward, ed. Tulsa, OK: Society of Exploration Geophysicists. 1990.

Danielson, R.E., and P.L. Sutherland. Porosity. *Methods of Soil Analysis. Part 1: Physical and Mineralogical Methods.* 2nd Edition. Number 9 (Part 1) in series Agronomy. A. Klute, ed. Madison, WI: Soil Science Society of America, Inc. 1986.

Dullien, F.A. *Porous Media: Fluid Transport and Pore Structure*. 2nd Edition. San Diego, CA: Academic Press, Inc. 1991.

Garabedian, S.P., L.W. Gelhar, and M.A. Celia. *Large-Scale Dispersive Transport in Aquifers: Field Experiments and Reactive Transport Theory.* Report 315. Cambridge, MA: Ralph M. Parsons Laboratory, Department of Civil Engineering, Massachusetts Institute of Technology. 1988.

Garabedian, S.P., D.R. LeBlanc, L.W. Gelhar, and M.A. Celia. Large-scale natural gradient tracer test in sand and gravel, Cape Cod, Massachusetts. 2: Analysis of spatial moments for a nonreactive tracer. *Water Resources Research* 27(5): 911–924. 1991.

Garnier, J.M., N. Crampon, C. Preaux, G. Porel, and M. Vreulx. Tracage par ^{13}C, ^{2}H, I^- et uranine dans la nappe de la craie sénonienne et écoulement radial convergent (Béthume, France). *Journal of Hydrology Amsterdam* 78: 379–392. 1985.

Gonzalez, D.D., and H.W. Bentley. Field test for effective porosity and dispersivity in fractured dolomite, the WIPP, Southeastern New Mexico. *Groundwater Hydraulics.* J. Rosenshein and G.D. Bennett, eds. *Water Resources Monograph 9.* Washington, DC: American Geophysical Union: 207–221. 1984.

Hess, K.M., S.H. Wolf, and M.A. Celia. Large-scale natural gradient tracer test in sand and gravel, Cape Cod, Massachusetts. 3: Hydraulic conductivity variability and calculated macro-dispersivities. *Water Resources Research* 28(8): 2,011–2,027. 1992.

Illman W.A., D.L. Thompson, V.V. Vesselinov, G. Chen, and S.P. Neuman. *Single- and Cross-Hole Pneumatic Tests in Unsaturated Fractured Tuffs at the Apache Leap Research Site: Phenomenology, Spatial Variability, Connectivity and Scale.* NUREG/CR–5559. Washington, DC: Nuclear Regulatory Commission. 1998.

Keys, W.S. *Borehole Geophysics Applied to Ground-Water Investigations.* Westerville, OH: National Groundwater Association. 1989.

Klinkenberg, L.J. The permeability of porous media to liquids and gases. American Petroleum Institute. *Drilling and Production Practice*: 200–213. 1941.

LeBlanc, D.R., S.P. Garabedian, K.M. Hess, L.W. Gelhar, R.D. Quadri, K.G. Stollenwerk, and W.W. Wood. Large-scale natural gradient tracer test in sand and gravel, Cape Cod, Massachusetts. 1: Experimental design and observed tracer movement. *Water Resources Research* 27(5): 895–910. 1991.

LeCain, G.D. *Results from Air-Injection and Tracer Testing in the Upper Tiva Canyon, Bow Ridge Fault, and Upper Paintbrush Contact Alcoves of the Exploratory Studies Facility, August 1994 through July 1996, Yucca Mountain, Nevada.* U.S. Geological Survey Water Resources Investigations Report 98-4058. 1998.

LeCain, G.D., L.O. Anna, and M.F. Fahy. *Results from Geothermal Logging, Air and Core-Water Chemistry Sampling, Air-Injection Testing and Tracer Testing in the northern Ghost Dance Fault, Yucca Mountain, Nevada, November 1996 to August 1998.* U.S. Geological Survey Water Resources Investigations Report 99-4210. 1999.

MacKay, D.M., D.L. Freyberg, and P.V. Roberts. A natural gradient experiment on solute transport in a sand aquifer. 1: Approach and overview of plume movement. *Water Resources Research* 22(13): 2,017–2,029. 1986.

Maloszewski, P., and A. Zuber. Mathematical modeling of tracer behavior in short-term experiments in fissured rocks. *Water Resources Research* 26(7): 1,517–1,528. 1990.

Massmann, J.W. Applying groundwater flow models in vapor extraction system design. *Journal of Environmental Engineering* 115(1): 129–149. 1989.

Massmann, J.W., and M. Madden. Estimating air conductivity and porosity from vadose-zone pumping tests. *Journal of Environmental Engineering* 120(2): 313–328. 1994.

Moench, A.F. Double-porosity models for a fissured groundwater reservoir with fracture skin. *Water Resources Research* 20(7): 831–846. 1984.

Moench, A.F. Convergent radial dispersion in a double-porosity aquifer with fracture skin: Analytical solution and application to a field experiment in fractured chalk. *Water Resources Research* 31(8): 1,823–1,835. 1995.

Neuman, S.P. Effect of partial penetration on flow in unconfined aquifers considering delayed gravity response. *Water Resources Research* 10: 303–312. 1974.

Neuman, S.P. Analysis of pumping test data from anisotropic unconfined aquifers considering delayed gravity response. *Water Resources Research* 11: 329–342. 1975.

Neuman, S.P. Perspectives on "delayed yield". *Water Resources Research* 15: 899–908. 1979.

Novakowski, K.S. An evaluation of the boundary conditions for one-dimensional solute transport: 1: Mathematical development. *Water Resources Research* 28(9): 2,399–2,410. 1992.

Novakowski, K.S., and P. Lapcevic. Field measurement of radial solute transport in fractured rock. *Water Resources Research* 30(1): 37–44. 1994.

Novakowski, K.S., and G. van der Kamp. The radial diffusion method. 2: A semianalytical model for the determination of effective diffusion coefficients, porosity, and adsorption. *Water Resources Research* 32(6): 1,823–1,830. 1996.

Page, J.B. Advantages of the pressure pycnometer for measuring the pore spaces in soils. *Soil Science of America Proceedings* 12: 81–84. 1948.

Reimus, P.W., and H.J. Turin. *Results, Analyses, and Interpretation of Reactive Tracer Tests in the Lower Bullfrog Tuff at the C-Wells, Yucca Mountain, Nevada.* Yucca Mountain Site Characterization Project Report Milestone SP2370M4. Los Alamos, NM: Los Alamos National Laboratory. 1997.

Rojstaczer, S., and J.P. Tunks.. Field-based determination of air diffusivity using soil air and atmospheric pressure time series. *Water Resources Research* 31(12): 3,337–3,343. 1995.

Rousseau, J.P., C.L. Loskot, F. Thamir, and N. Lu. *Results of Borehole Monitoring in the Unsaturated Zone within the Main Drift Area of the Exploratory Studies Facility, Yucca Mountain, Nevada.* Yucca Mountain Project Level 3 Milestone Report SPH22M3. Las Vegas, NV: Yucca Mountain Project Office. 1997.

Russell, M.B. A simplified air picnometer for field use. *Soil Science of America Proceedings* 14: 73–76. 1950.

Shan, C. Analytical solutions for determining vertical air permeability in unsaturated soils. *Water Resources Research* 31(9): 2,193–2,200. 1995.

Shan, C., I. Javandel, and P.A. Witherspoon. Characterization of leaky faults: Study of air flow in faulted vadose zones. *Water Resources Research* 35(7): 2,007–2,013. 1999.

Sharma, P.V. *Environmental and Engineering Geophysics.* New York: Cambridge University Press. 1997.

Stallman, R.W. Flow in the Zone of Aeration. *Advances in Hydroscience.* Ven Te Chow, ed. New York: Academic Press 4:151–195. 1967.

Stallman, R.W., and E.P. Weeks. The use of atmospherically induced gas-pressure fluctuations for computing hydraulic conductivity of the unsaturated zone. *Geological Society of America, Abstracts with Programs* 7: 213. 1969.

Streltsova, T.D. Drawdown in compressible unconfined aquifers. Proceedings of American Society of Civil Engineers. *Journal of Hydraulic Division* 10(HY11): 1,601–1,616. 1974.

Telford, W.M., L.P. Geldart, R.E. Sheriff, and D.A. Keys. *Applied Geophysics.* New York: Cambridge University Press. 1976.

van der Kamp, G., D.R. Van Stempvoort, and L.I. Wassenaar. The radial diffusion method. 1: Using intact cores to determine isotopic composition, chemistry, and effective porosities for groundwater in aquitards. *Water Resources Research* 32(6): 1,815–1,822. 1996.

Vesselinov, V.V., and S.P. Neuman. Numerical inverse interpretation of multistep transient single-hole pneumatic tests in unsaturated fractured tuffs at the Apache Leap Research Site. *Theory, Modeling and Field Investigations in Hydrogeology: A Special Volume in Honor of Shlomo P. Neuman's 60th Birthday.* Boulder, CO: Geological Society of America. 2000.

Vukovíc, M., and A. Soro. *Determination of Hydraulic Conductivity of Porous Media from Grain-Size Composition.* Littleton, CO: Water Resources Publications. 1992.

Weeks, E.P. *Field Determination of Vertical Permeability to Air in the Unsaturated Zone.* U.S. Geological Survey Professional Paper 1051. 1978.

Wolf, S.H. *Spatial variability of hydraulic conductivity in a sand and gravel aquifer.* Engineering Thesis, Massachusetts Institute of Technology, Department of Civil Engineering, Cambridge, MA. 1988.